Volume 39, Number 4, 2013.

Mobility & Vehicle Mechanics

International Journal for Vehicle Mechanics, Engines and Transportation Systems

ISSN 1450 - 5304

UDC 621 + 629(05)=802.0

UNIVERSITY OF KRAGUJEVAC, FACULTY OF ENGINEERING

SERBIAN SOCIETY OF AUTOMOTIVE ENGINEERS

M V M **M**obility **V**ehicle **M**echanics

*Editors: Prof. dr **Jovanka Lukić**; Prof. dr **Čedomir Duboka***

MVM *Editorial Board*
University of Kragujevac
Faculty of Engineering
Sestre Janjić 6, 34000 Kragujevac, Serbia
Tel.: +381/34/335990; Fax: + 381/34/333192

For Publisher: Prof. dr Miroslav Živković, dean, University of Kragujevac, Faculty of Engineering

Publishing of this Journal is financially supported from:
Ministry of Education, Science and Technological Development, Republic Serbia

Mobility & **V**ehicle **M**echanics

Motorna **V**ozila i **M**otori

Volume 39
Number 4
2013.

Mobility & **V**ehicle **M**echanics

Motorna **V**ozila i **M**otori

Volume 39
Number 4
2013.

STRESS AND DEFORMATION ANALYSIS FOR THE LOWER KNUCKLE BRACKET OF FRONT SHOCK ABSORBERS

Ionel Vier [1], Viorel Nicolae, Danut-Gabriel Marinescu, Adrian Rosescu, Gheorghe Petrache

UDC:629.3.01

ABSTRACT: This paper presents a comparative analysis of the stresses and deformations for different constructive solutions of lower knuckle bracket of the damper fitting a front axle Mac Pherson type. As calculation method we used the Finite Element Method (FEM) and as software we used CATIA v5. The analyse was performed under static conditions, using forces parallel to the longitudinal and transverse directions of the car.

KEYWORDS: static analysis, shock absorbers, CATIA V5, CAE, FEM

NAPONSKO DEFORMAIONA ANALIZA DONJE UŠKE PREDNJEG AMORTIZERA

REZIME: Rad prikazuje uporednu analizu napona i deformacija za različita konstruktivna rešenja donje uške amortizera McPherson-ovog oslanjanjs prednje osovine. Korišćena je računska metoda konačnih elemenata (FEM) i programski paket Catia v5 . Analiza je urađena u statičkim uslovima gde su sile bile pralelne použnom poprečnom pravcu vozila.

KLJUČNE REČI: statička analiza, amortizer, Catia v5, metoda konačnih elemenata MKE, računarski podržano inženjerstvo

[1] *Received September2012,Accepted October 2012*

Intentionally blank

STRESS AND DEFORMATION ANALYSIS FOR THE LOWER KNUCKLE BRACKET OF FRONT SHOCK ABSORBERS

Ionel Vier[1], Viorel NicolaE, Danut-Gabriel Marinescu, Adrian Rosescu, Gheorghe Petrache

UDC: 629.3.01

INTRODUCTION

This paper presents a study on the lower knuckle bracket of a shock absorber used in a Mac Pherson type front suspension.

It was studied the influence of the thickness reduction of the bracket's plate material. Its thickness was changed from 3.5 mm to 3 mm. Because the bracket's shape is relatively complex (Figure 1), there were analyzed with priority its deformations in two directions, longitudinal and transverse. There were done two types of analysis, one performed on a simple piece (Figure 1) and another on the whole assembly (Figure 2).

The analysis of the the simple piece used rigid elements to simulate the action of the force, and for the whole assembly it was properly applied a force to the damper tube. Thus for comparison on the two directions (OX and OY - longitudinal and transverse) there were applied forces of 1000 N.

The CATIA V5 software was used for modeling and making the analyse, the calculation was carried out in the static regime using the "Generative Structural Analysis" module of the software [2].

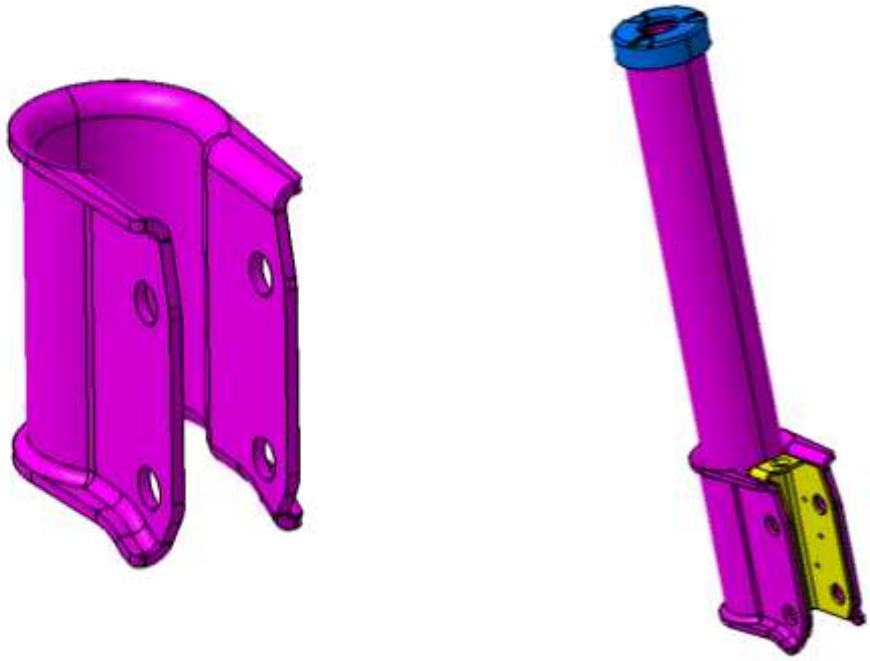

a) The lower knuckle bracket of the shock absorber. *b) The assembly used for calculation.*

Figure 1. The CAD 3D models.

[1] *Ionel VIERU, University of Pitesti, Romania, ionel.vieru@upit.ro*

THE CALCULATION MODEL

If the first comparative analysis, for the simple part we loaded the model using rigid elements (option "smooth virtual part" of CATIA) from the point of application of force to the lower knuckle bracket of the shock absorber for two situations of the piece thickness: 3.5 mm and 3.0 mm [1].

The forces were applied consecutively on OX and OY directions, and the recessed was applied to the mounting holes, as shown in figures 2a and 2b.

a) The force on the OX direction (longitudinal plane) *b) The force on the OY direction (transversal plane)*

Figure 2. The forces applied on the simple element.

The result is a model with a total of 21,507 nodes and a total of 10,793 parabolic octree tetrahedron. It was also done an analyse on the shock absorber assembly for the two cases (3.5 mm plate thickness and 3 mm plate thickness), using the same load of 1000 N size on the two directions (OX and OY) applied at the shock tube end, as shown in Figure 3.

The result is a model with a total of 102,435 nodes and a total of 56,045 octree tetrahedron of parabolic type. In both cases, the material properties used in calculation are given in Table 1.

a) The force on the OX direction (longitudinal plane)

b) The force on the OY direction (transversal plane)

Figure 3. The forces applied on the shock absorber assembly .

Table 1. *The properties of the material.*

Material	Steel
Young's modulus	2e+011N_m2
Poisson's ratio	0.266
Density	7860kg_m3
Coefficient of thermal expansion	1.17e-005_Kdeg
Yield strength	2.5e+008N_m2

RESULTS AND CONCLUSIONS

For each load case there were calculated and analyzed the displacements (δ) and additional there were calculated the von Mises stress (σ).

Table 2 presents the results of calculations for the single part and Table 3 summarized the results for the shock absorber assembly.

Table 2. *The results obtained on the single part.*

Force, [N]	Part with 3,5 mm thickness		Part with 3,0 mm thickness	
	δ [mm]	σ [MPa]	δ [mm]	σ [MPa]
X = 1000	0,55	293	0,71	382
Y = 1000	0,23	138	0,30	160

Table 3. *The results obtained on the shock absorber assembly.*

Force [N]	Part with 3,5 mm thickness		Part with 3,0 mm thickness	
	δ [mm]	σ [MPa]	δ [mm]	σ [MPa]
X = 1000	0,75	212	0,80	246
Y = 1000	0,56	118	0,55	129

Figures 4 and 5 present the displacements and the von Mises stress, the force being applied by the direction of OX axis.

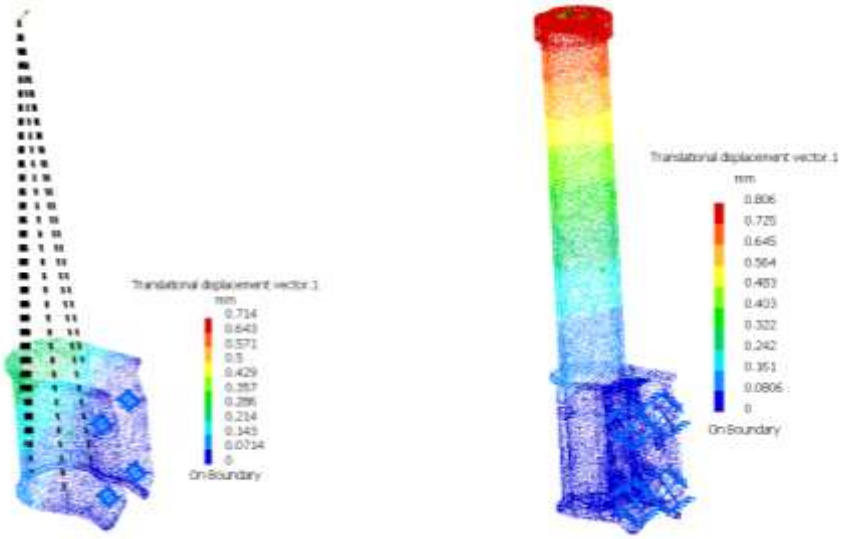

a) Single part *b) Shock absorber assembly*

Figure 4. The displacements obtained for the material with 3,0 mm thickness with the force applied by the direction of OX axis.

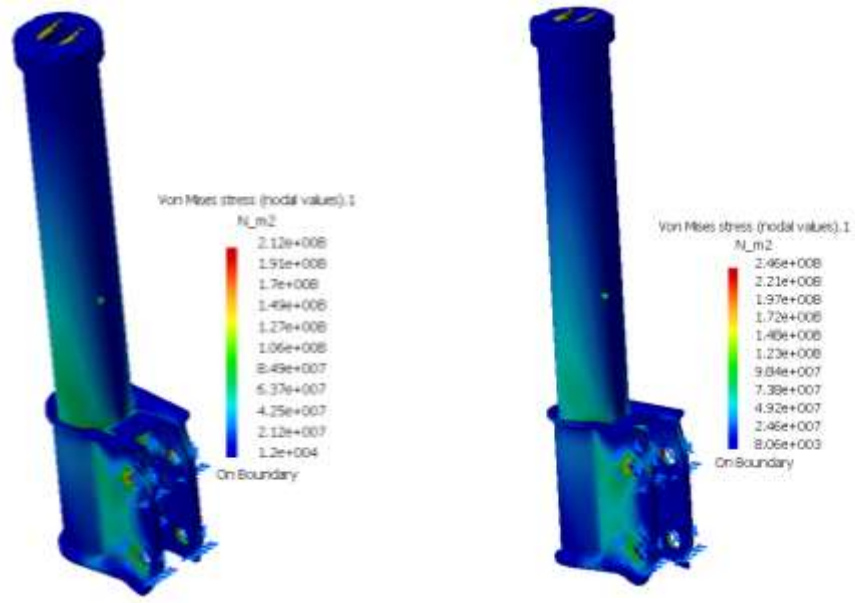

a) Shock absorber assembly with 3.5 mm thickness *b) Shock absorber assembly with 3.0 mm thickness*

Figure 5. The von Mises stress *obtained with the force applied by the direction of OX axis.*

Analyzing the results presented in Tables 2 and 3, we observe that on the OX axis direction the displacements are higher than those on the OY axis direction, in both cases analyzed.

It also finds that even on the single part could be observed differences of displacements, especially on the OX axis, the overall differences are much smaller, leading to the same values of rigidities for the two variants.

In conclusion, when using the material with thickness of 3.0 mm it is obtained a behavior almost similar with the one obtained when using the material with thickness of 3.5 mm, corresponding to a mass reduction of about 0.080 kg. This conclusion was practically confirmed by the attempts to validate the shock absorber [3].

REFERENCES

[1] Vieru, I., Popa, D., Popa, C., Elemente de bază ale proiectării asistate de calculator, Editura Universităţii din Piteşti, 2005.
[2] * * * - CATIA V5 documentation.
[3] * * * RENAULT documentation for front shock absorbers.

CALCULUS AND CONSTRUCTION OF A LASER PLUG

Dejanu Marcel[1], *Dascălu Traian, Popa Dinel, Parlac Sebastian, Salamu Gabriela*

UDC: 662.6

ABSTRACT: In the paper are presented the stages that led to the construction of a laser plug. This laser plug has the dimensions of a classical spark plug that is used at spark ignition engines. The determinations of the optimal pumping characteristics, the length of the optical resonator, the pumping energy etc. were realized after a set of experiments conducted in a static enclosure. The main characteristics of the laser and optical system were determined. The pumping mechanism is made of a laser diode that is coupled to a fiber optic. The end of the optical fiber is coupled to a Nd:ZAG crystal through an achromatic collimation system, the duration of the laser pulse being of 100 Hz. During the test one concluded that the laser functions in the initial parameters of -60°C and 150°C.

KEYWORDS: laser plug, optical system, laser diode, fiber optics, static enclosure.

PRORAČUN I KONSTRUKCIJA LASERSKOG UPALJAČA

REZIME: U radu su prikazene faze konstrukcije laserskog upaljača. On ima dimenzije klasične svećice koja se koristi kod motora sa paljenjem varnicom. Određivanje optimalne karakteristike ubrizgavanja, dužine optičkog rezonatora, potrebna energina pobuđivanja medijuma, itd. je realizovana pošto su izvedeni eksperimenti u statičkom okruženju. Najvažnija karakteristika laserskog i optičkog sistema je određena. Mehanizam ubrzgavanja je napravljen od laserske diode koja je povezana optičkim vlaknima. Kraj optičkog vlakna je optičkovlakno povezano sa Nd:ZAG kristalom kroz ahromatski kolimacioni system, trajanje laserskog pulsa počinje od 100 Hz. Tokom testa izveden je zaključak da uloga lasera je značajna u polaznoj fazi između -60°C i 150°C.

KLJUČNE REČI: laserski upaljač,optički system, laserska diode, optičko vlakno, statički uslovi.

[1] *Received September 2012, Accepted October 2012.*

Intentionally blank

CALCULUS AND CONSTRUCTION OF A LASER PLUG

Dejanu Marcel , Dascălu Traian,Popa Dinel, Pârlac Sebastian, Salamu Gabriela

UDC:662.6

INTRODUCTION

The domain of the presented paper is an interdisciplinary domain. For one to make an integrated system that can ignite fuel mixtures using a laser pulse one has to unite at least two domains of the sciences: the Physics and the Mechanical Engineering.

The domain of lasers physics began once with the patenting of the first laser device (1958). After a first period, the theoretical development of the domain, a second period began where laser construction also developed. Even though laser impulse ignition systems were never used on a series production many great automotive companies are conducting studies regarding laser ignition in heat engines and we are confident that the future of these systems is not far from here. As evidence, these kind of systems already have miniature dimensions, high reliability and a low production cost.

The type of lasers developed until now presents a large spectrum of physical and operational parameters. If one categorizes laser types, then one will have lasers: with solid, liquid or gas active environment. If lasers are categorized by the length wave of the emitted radiation, then one will have: infrared lasers, visible lasers, ultraviolet lasers and X rays lasers.

The process through out atoms are lifted from one energy level to another is called pumping. Normally, this kind of process can take place in three different ways:

- optical pumping, for example, by absorbing the light emitted by a powerful lamp or another laser,

- electrical pumping, for example, by keeping the atoms (molecules) in a radio-frequency field or by injecting electrical current into an active semiconductor environment,

- chemical pumping, for example, an exothermic chemical reaction.

For an efficient pumping, the light emitted by the diode system must be transferred into an active environment in a proper manner. There are two types of pumping geometries: longitudinal pumping, where the pumping beam enters the laser environment along the resonator axis and transversal pumping, where the pumping beam is transferred in the active environment through different directions that are perpendicular to the optic resonator axis.

In the case of longitudinal pumping, the beam emitted by the laser diode has to be focalized in the active environment, in a portion of $100\,\mu m - 1\,mm$.

In the case of transversal pumping, the active environment, shaped in a bar, plate or disc shape, can be operated efficiently with at a high pumping power. There are a lot of pumping configurations but we will present two cases that are fitted best with our experiment. The first case presents a bar of $Nd:YAG$ with the diameter of $4\,mm$, cooled through the use of water that runs through the tube that surrounds it, that is radially pumped by three or five modules placed into a circular arrangement. The transfer efficiency of this one is estimated at $\sim 80\%$. For one to increase the efficiency, reflectors of the pumping radiation are placed around the $Nd:YAG$ bar, opposing the pumping diodes. This arrangement produces $\sim 600W$, output power with an optical efficiency of $\sim 25\%$. A second transversal pumping configuration is fir microchip lasers made of a composite

material called $Yb:YAG/YAG$. The thickness of the active environment is of $200-400\,\mu m$ and it is made of a central zone made of $Yb:YAG$, $10\,at\%Yb$, having the section of $2\,mm\times 2\,mm$ surrounded by undoped YAG, the total diameter being of $10\,mm$. The pumping radiation that is introduced through the edge of the microchip is propagated through total internal reflection in the undoped area and it is absorbed in the doped area.

THE LASER PLUG CONSTRUCTION

LASER PLUG BODY

Using the theoretically knowledge regarding the pumping diagrams, also based on the experiments previously conducted in the lab, one can now move to construct a laser plug with the dimensions similar to the one of a classical spark plug.

The functioning diagram of the experimental montage for the laser plug is presented in figure 1 and has the following composure: a Nd:YAG crystal, the S1 surface covered with an anti-reflex layer that has a transmitting coefficient of T>0,998 of a length wave of λem=1064 nm.

The S2 surface is covered with anti-reflex at 1064 nm. The Cr4+:YAG crystals used in our study have different initial transmitting coefficients, both surfaces S1 and S2 of the saturable absorbers crystals, SA are treated for anti-reflex on the length wave of λ=1064 nm; a high reflectivity mirror HRM is placed at the entrance of the pumping wave λP and is focalized with a lens system L1 and L2. A second crystal with saturable absorbers, SA - Cr4+:YAG is situated near the exit of the mirrors system (OCM) or at the edge of surface S2 of the Nd:YAG crystal. Under these circumstances, the length of the resonator cannot be reduced under 60 mm.

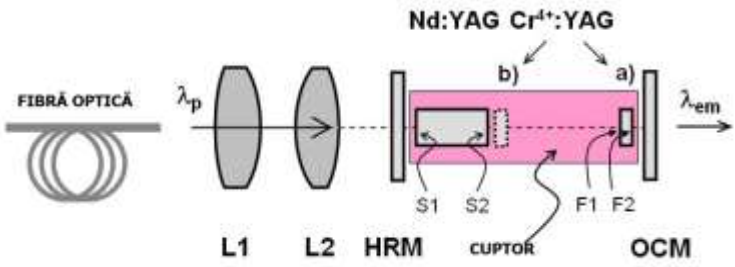

Figure 1. Functional scheme of Nd laser spark: YAG/Cr4 +: YAG.

The pumping system is made of a laser diode whose radiation is coupled to a fiber optic. The end of the fiber optic is virtually coupled to the Nd:YAG crystal through an achromatic collimation system made out of the lenses L1 and L2.

The energy of the laser pulse was determined by using an energy measuring device type Laser Probe RJP-445 and the wideness of the pulse was determined using a Thorlabs SV 2 photodiode type FC with the reaction time of 0,2 ns.

The functioning of the laser plug was experimentally tested at temperatures between 25^0C and 150^0C, and it was concluded that the output performances of the system does not modify with the temperature. In the literature [Xiao, G., Lim, J.H., Yang, E.,

Stryland, V., Bass, M., Weichman, L., IEEE J. Quantum Electron, 1086 (1999)], are presented paper where similar pumping systems and laser emission are stable in the range of - 60^0C to +90^0C.

A constructive solution with a single-block resonator was used so that can all the mechanical adjusting components for adjusting the position of the reflecting surfaces to be eliminated (the mirrors from figure 2). Practically, a 10 mm cylindrical active environment was used with a composite structure; the active environment and the saturable absorber are glued together through high temperature optical diffusion.

The mechanical design process has as purpose to achieve a mechanical montage capable of resisting shocks and mechanical vibrations without modifying its functionality and that also can include the laser and the collimation and focalization components into a single mechanical ensemble with the maximum length of 7,62 cm.

The constructive diagram is component explode detailed in figure 2. Finally, a laser plug was obtained comparable with the sizes of a classical one, as you can see in the pictures from figure 3.

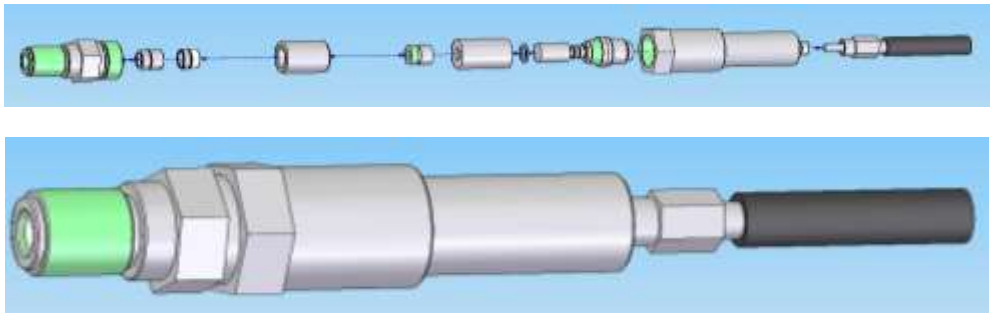

Figure 2. The constructive scheme of the laser plug.

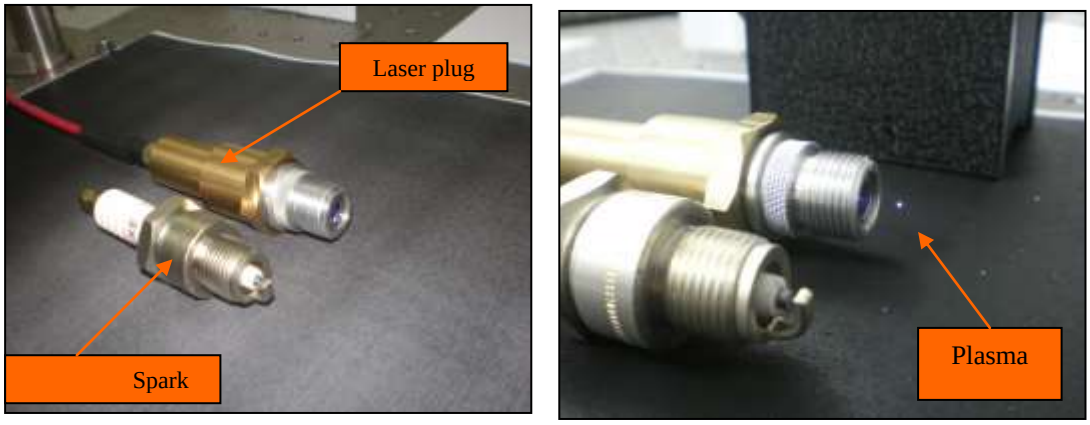

Figure 3. Dimensions of laser spark plug versus a classical electrical spark plug.

THE PUMPING SYSTEM

In figure 4 is presented the pumping and transmitting device to the plug of the pumping laser pulse. The equipments are fixed on a special laboratory surface table that

assures modularly montage procedures, according to the necessities of the experiment. All illustrations, photos, graphics, etc. must be embedded as Figures into the document. Separate graphic files are not accepted. Line art must be professionally drawn and photos must be high quality with adequate contrast.

The research must proceed with the specification of the proper characteristics for the use of equipments in the automotive domain. In figure 4 one can identify the following components: (1) the power supply of the laser diode; (2) the pumping ensemble of diodes; (3) the optical transmitting system of the laser pulse to the fiber optics; (4) fiber optics; (5) laser plug.

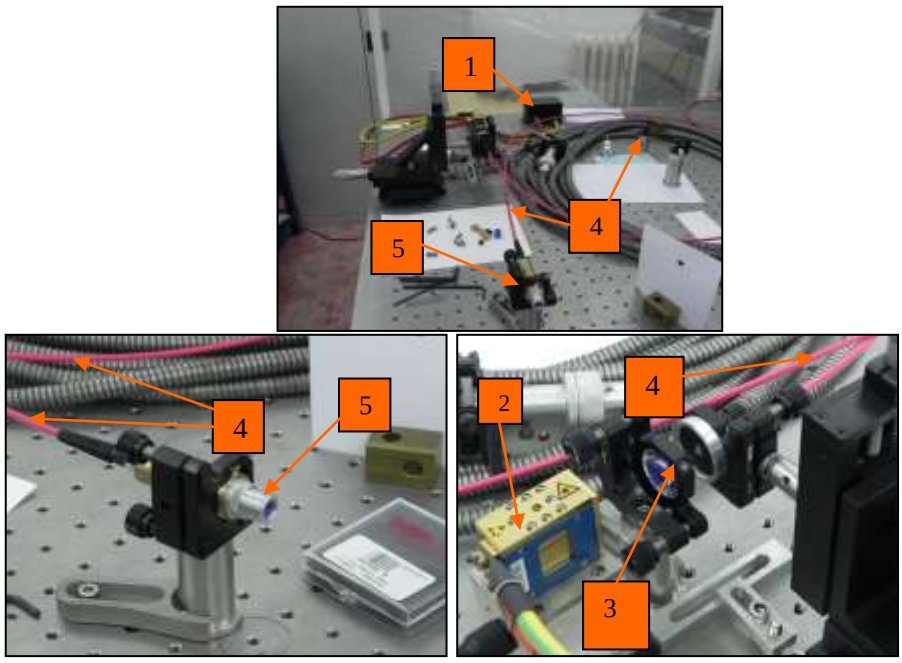

Figure 4. The components of the system of the pumping laser pulse beam.

THE UNFOLDING OF THE LASER PLUG IGITION EXPERIMENTS

GENERALITIES

In this stage of the experiments some research were conducted considering initiating the ignition of a methane-air fuel mixture having different concentrations (6%, 8%, 10% synthetic methane – air) by using the two ignition systems: a - the classical spark plug ignition; and b - the laser plug ignition.

During the experiments different parameters of the burning process were determined, such as: peak pressure, the variation of pressure through time, flame front propagation velocity, all of this conducted for different initial pressures and different values of the laser pulse energy.

Finally, one proceeds to a comparative analysis of the laser ignition with the classical spark plug ignition of the fuel mixture.

DESCRIBING THE EXPERIMENTAL BENCH

The experimental montage used for the experiments is described in figure 5 where:

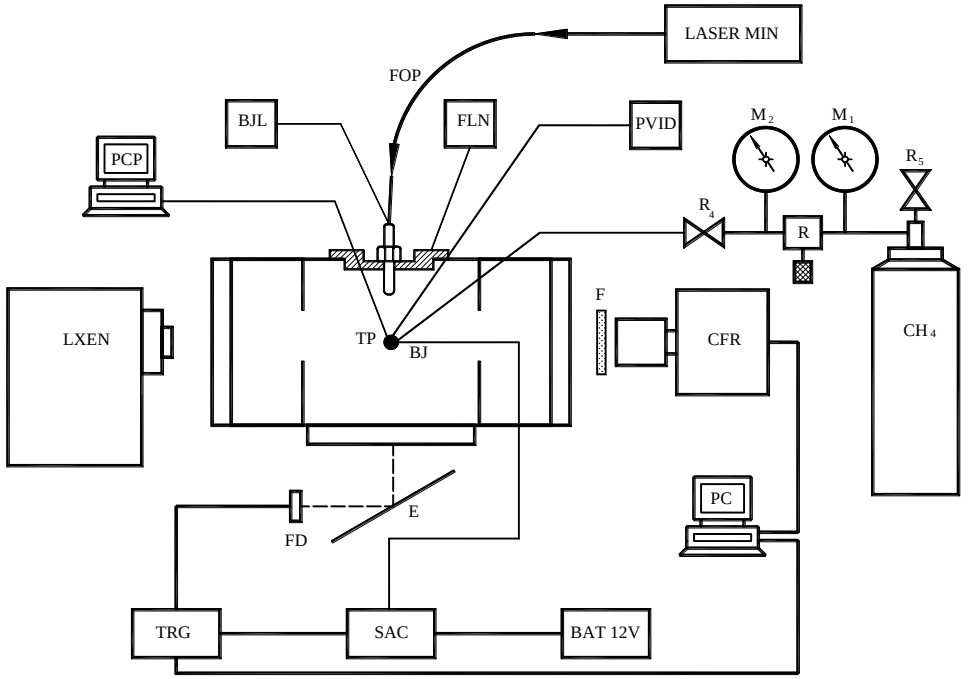

Figure 5. The scheme of the experimental bench with laser plug.

LASER MIN - is a miniature laser with a solid body Nd:YAG, pumped with laser diodes that are passively commuted with Cr^{4+}:YAG" (Nd:YAG/Cr^{4+}:YAG; BJL- is a laser spark plug that focalizes the laser pulse inside the static chamber and starts the burning process of the fuel mixture; LXEN - is a XENON lamp that assure the illumination of the burning phenomenon's from inside the chamber, in order to assure perfect view for the images recorded in shadowgraph method; FD - is the photodiode with a role of commanding the trigger system; E - is the screen for capturing the light signal, the light signal is recognized by the photodiode; CFR - is a rapid filming video camera; F - the protection filter for protecting the radiation incidence with λ=1064 nm in the camera; PC - is the computer with a software dedicated to process the images transmitted by the rapid filming video camera (CFR); FOP - is the optical fiber that transmits the laser pulse from the emitter to the plug; FLN - is the surface that assures the montage of the laser plug on the static chamber; PCP-TP - is the measuring and recording equipment for pressure variations.

The experimental bench is presented in figure 6 where: (1) is the static chamber; (2) is the rapid filming video camera; (3) is the XENON lamp; (4) - is the contrivance that assures the montage of the laser plug on the static chamber; (5) is the laser plug; (6) is the pressure regulator; (7) is the optical fiber that transmits the laser pulse from the emitter to the plug.

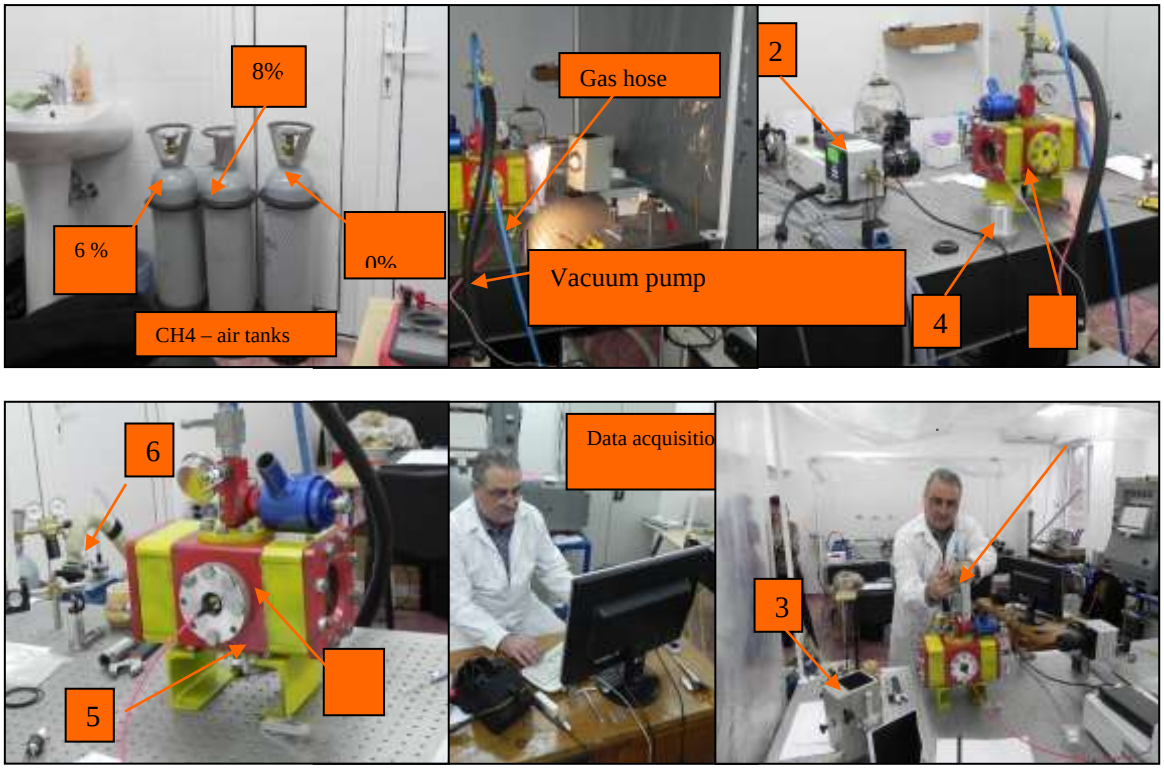

Figure 6. The physical experimental bench of the laser plug ignition system.

In order to apply the "shadowgraph" method for capturing images of the flame front propagation process, a xenon illuminating lamp was used. The Xenon lamp facilitates the illumination of the burning phenomenon's from inside the chamber, in order to assure a perfect view for the images recorded in shadowgraph method. A photodiode commands the beginning of the recording process when the burning process is initialized. The images are recorded with a rapid filming video camera type **"**PHOTRON – FASTCAM 1024 PCI**".** The recordings were taken at a velocity of 3000 frames/second at a resolution of 512 x 512 pixels. The images are captured by a data acquisition system under the form of photographs of the expanding flame front that are then processed by a PC dedicated to this kind of operation.

DESCRIBING THE EXPERIMENTAL RESULTS

Have been carried out experiments of ignition the methane-air fuel mixture burning process for three types of concentration of methane in synthetically air and for different types of initial pressure from the combustion chamber, as it is presented:

- for conventional spark plug ignition at initial pressures of 6%, 8% and 10% CH_4-air,
- for laser plug ignition at initial pressures of 6%, 8% and 10% CH_4-air.

In figures 7 and 8 are comparatively presented the flame front propagation velocity for all the experimental cases. In figure 9 are presented the photographs of the flame front

evolution for the methane-air concentrations: 8% concentration - Pi = 5 bar, 8% concentration - Pi = 5,5 bar, laser ignition.

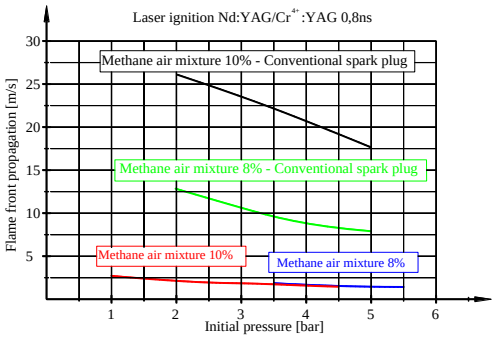

Figure 7. The flame front velocity variation depending on the initial pressure of the comparative fuel mixture - ignited with conventional and laser plug.

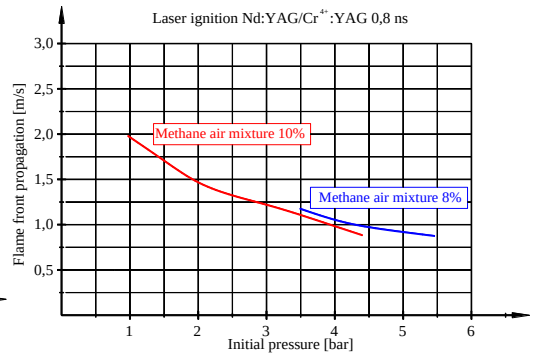

Figure 8. The flame front velocity variation depending on the initial pressure of the fuel mixture, in the case of laser ignition.

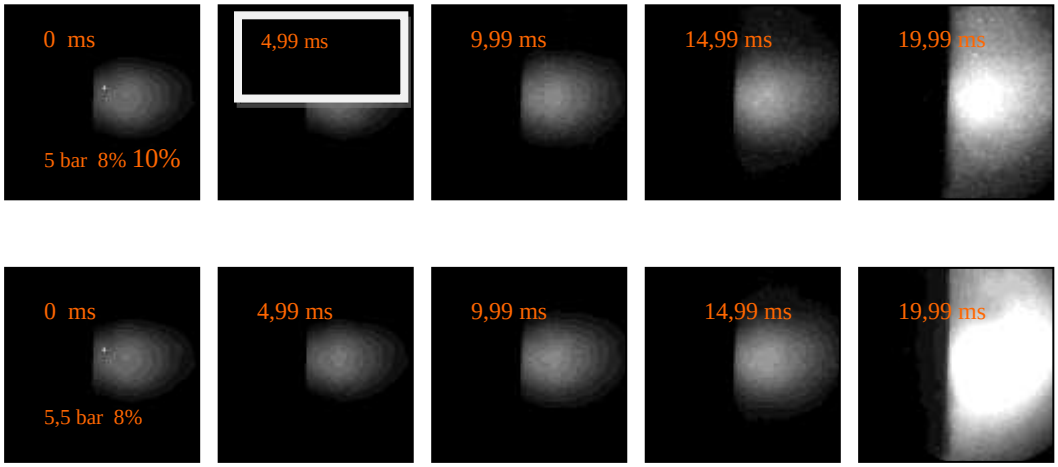

Figure 9. The evolution through time of the flame front for the methane-air mixture with the following characteristics: 8% concentration - Pi = 5 bar; 8% concentration - Pi = 5,5 bar ; laser ignition.

In figure 10 one presents the evolution of the flame front propagation for the methane-air fuel mixture with the following concentrations: 8% concentration - Pi = 4 bar; 8% concentration - Pi = 5,5 bar ; conventional electrical plug ignition.

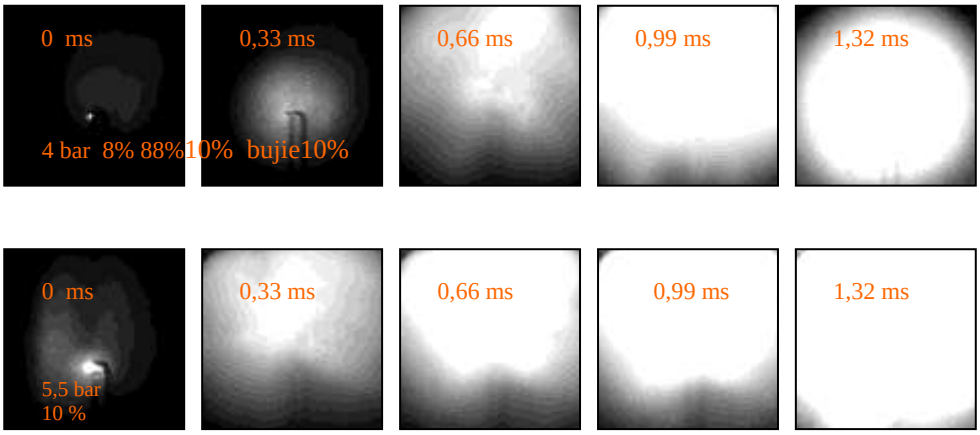

Figure10. The evolution of the flame front propagation for the methane-air fuel mixture with the following concentrations: 8% concentration - Pi = 4bar; 8% concentration - Pi = 5,5bar; electrical spark ignition.

In figure 11 it is presented the graph that describes the maximum pressure variation that is obtained in the combustion chamber depending on the initial pressure for a fuel mixture of 8% methane-air.

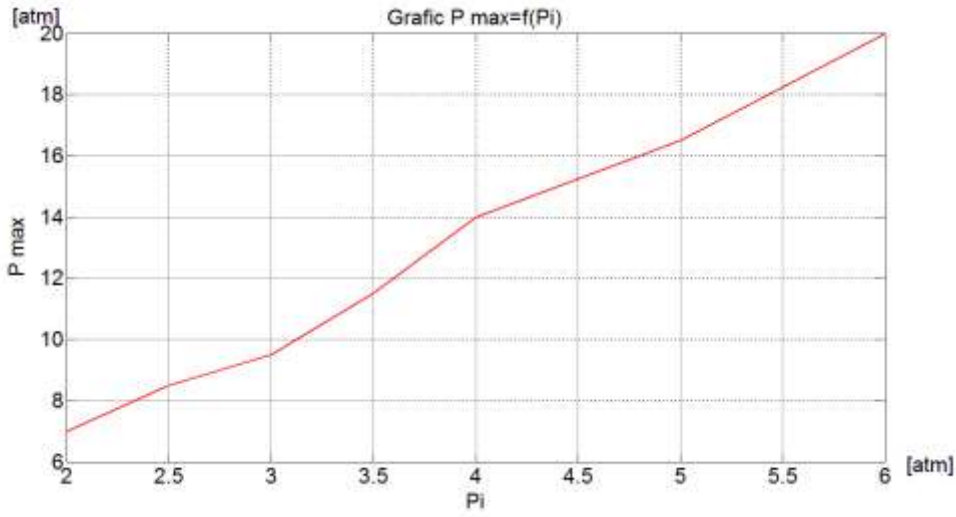

Figure 11. Maximum pressure evolution depending on the initial pressure.

CONCLUSIONS THAT RESULTED FROM THE EXPERIMENTS

From the experiments conducted in this stage of the research one concluded the following things: the laser plug type Nd:YAG/Cr4+:YAG, having the characteristics: 1ns pulse duration, pulse frequency of 5 Hz, the energy of 3 mJ, the wavelength of $\lambda = 1064$

nm, can ignite methane-air fuel mixtures for different concentrations and initial pressures in the combustion chamber.

It was proven experimentally that the ensemble laser emitter - laser plug is stable at temperatures in the range of -60^0 to $+ 150^0$C.

The laser pulse emission equipment can be made at real sizes, so it could be mounted on a vehicle, without any technical difficulties.

The laser plug can be made out of a case identical with the one of a spark plug so that it can be mounted on the engine without any other modifications.

The fiber optics permits the laser pulse to be transmitted from the emission equipment to the laser plug, on any distance, just by avoiding the accentuated angularly strangling condition. As a result, the emission equipment can be mounted inside the vehicle from where the laser pulse can be transmitted through fiber optics to the laser plugs mounted on the engine, without any other technical difficulties or special ensembles.

After a relatively small number of pulses the lenses from inside the chamber are covered with smoke, process that diminishes the energy of the discharge pulse. Solving this inconvenient represents a major research direction that will shape the future of the laser plugs on the internal combustion engines from the product series.

The conducted experiments proves the opportunity for creating and perfecting laser equipments that could be tested in real functioning conditions, on an engine and on a vehicle.

REFERENCES

[1] Beduneau, J.,L,, Kim, B., Zimmer, L., Ikeda, Y., Measurements of minimum ignition energy in premixed laminar methane/air. Now by using laser induced spark, Combust Flame, 2003;132:653–65.

[2] T Bindhu, C.,V., Harilal, S.,S., Tillack, M.,S., Najmabadi, F., Gaeris, A.,C., Laser propagation and energy absorption by an argon spark, Journal of Applied Physics 2003;94(12):7402–7.

[3] Dascalu, T., Dascalu, C., Physics Of Lasers ,Editura Printech, 2006.

[4] Dascalu, T., Pavel, N., High Temperature Operation of a Diode Pumped Passively Q Switched Nd:YAG/Cr4+:YAG Laser, Laser Physics, 2009, Vol. 19, No. 11, pp. 2090–2095.

[5] Dascalu, T., Philips, G., and Weber, H., Investigation on Cr4+ passive Q-switch in CW pumped Nd:YAG LASER, Optics & Laser Technology, .vol.29, no.3, p.145 (1997).

[6] Kofler a,H., Schwarz,E., Wintner, E.,Experimental development of a monolithic passively Q-switched diode-pumped Nd:YAG laser,) Eur. Phys. J. D 58, 209–218, 2010.

[7] Kopecek, H., Wintner, E., Lackner, M., Winter, F., Hultqvist, A., Laser-simulated ignition in a homogeneous charge compression ignition engine. SAE 2004-01- 0937 2004.

[8] Ma, J.,X., Alexander, D.,R., Poulain, D.,E., Laser spark ignition and combustion characteristics of methane–air mixtures, Combust Flame 1998;112:492–506.

[9] McNeill, D.,H., Minimum ignition energy for laser spark ignition, Proc. Combust. Inst. 30 (2005) 2913–2920.

[10] Mohamed, H., Ko, Y.,S., Chung, S.,H., An Experiment on the Combustion Characteristics with Laser-Induced Spark Ignition, KSME International Journal, Vol. 13, pp.82-89, 1999.

[11] Phuoc, T., X., Laser-induced spark for simultaneous ignition and fuel-to-air ratio measurements, Optics and Lasers in Engineering 44 (2006) 520–534, Pittsburgh, PA 15236, USA.
[12] Phuoc, T.,X., An experimental and numerical study of laser-induced spark in air, Opt. Laser Eng. 43 (2005) 113–129.
[13] Phuoc, T.X., Laser spark ignition: experimental determination of laser-induced breakdown thresholds of combustion gases, Opt. Commun. 175 (2000) 419–423.

EMISSION CHARACTERISTICS OF A DIESEL ENGINE USING BIODIESEL PRODUCED FROM RAPESEED OIL

Breda Kegl[1], *Stanislav Pehan, Marko Kegl*

UDC: 621.43

ABSTRACT: The paper discusses the influence of rapeseed oil on the engine emission characteristics. The treated engine is an industrial vehicle diesel engine with an injection M system. The considered fuels are various mixtures composed of conventional mineral diesel and rapeseed oil. The engine characteristics are obtained by numerical and experimental procedures. Various engine operating regimes are considered. Besides of the fuel composition, the injection pressure, in-cylinder gas pressure, ignition delay, and other engine working condition are varied and analysed. Consequently, the heat release rate, exhaust gas temperature, harmful emissions, specific fuel consumption, engine power spectra, and other engine performances are determined. Special attention is devoted to NOX-emissions due to the lower cylinder temperatures caused by several biofuel influencing factors.

KEYWORDS: Biodiesel, NOX Emission

KARAKTERISTIKE EMISIJE DIZEL MOTORA KOJI KORISTI BIODIZEL DOBIJEN OD ULJANE REPICE

REZIME: U radu je predstavljen uticaj uljane repice na karakteristiku emisije motora. Korišćen je industrijski dizel motor sa M sistemom za ubrizgavanje. Korišćena goriva su različite mešavine konvencionalnih mineralnih dizela biodizela od uljane repice. Karakteristike motora dobijene su računskim i eksperimentalnim putem. Posmatrani su različiti režimi rad motora. Pored smeše goriva, pritiska ubrizgavanja, pritiska gasa u cilindru, kašnjenja paljenja varirani su i drugi radni uslovi. Istovremeno su određivani i analizirani: brzina oslobađanja toplote, temperatura izduvnih gasova, emissija štetnih gasova, specifična potrošnja goriva, spektar snage motora i ostale performanse motora. Posebna pažnja je posvećena emisiji azotoksida nastalu smanjenjem temperature u cilindru što je rezultat nekoliko uticajnih faktora bio goriva.

KLJUČNE REČI: Bio-dizel, NOX emisija

[1] *Received September 2012, Accepted October2012*

Intentionally blank

EMISSION CHARACTERISTICS OF A DIESEL ENGINE USING BIODIESEL PRODUCED FROM RAPESEED

Breda Kegl, Stanislav Pehan, Marko Kegl

UDC:629.321

INTRODUCTION

To reduce harmful diesel engine emissions many experimental and numerical investigations related to the control of the injection and combustion processes have been done. To fulfill strongest emissions regulations many kinds of alternative fuels have been investigated.

The most frequently investigated parameters are related to the injection rate, injection timing, injection duration, injection pressure, start of combustion, in-cylinder gas pressure and temperature, and heat release rate. NOX emissions are significantly affected by injection timing and injection pressure [1]. Advanced injection timing and higher injection pressure result in higher in-cylinder gas temperatures. Soot emissions reduce as the injection pressure is increased and the minimum values are reached in case of advanced injection timing which improves the soot oxidation [1]. A strong relationship of the air/fuel ratio and in-cylinder gas temperature with NOX and soot emissions is reported [2]. To improve combustion and reduce harmful emissions of diesel engines, various oxygenates may be added to mineral diesel. The ignition delay influences the combustion process strongly [3, 4].

Biofuels may offer an opportunity to reduce some of the harmful emissions without expensive engine modifications. Biodiesel is a very promising fuel because it is a sulfur-free, non-toxic, oxygenated, renewable, and more than 90% biodiesel can be biodegradable within 3 weeks. Biodiesel has higher cetane number than mineral diesel, no aromatics, almost no sulfur, and contains more oxygen by weight.

Biodiesel distinguish higher density, viscosity, surface tension, sound velocity, and bulk modulus of elasticity. This affects the fuelling, injection timing, and fuel spray and consequently the emission characteristics [5]. The advantages of the biodiesel are shorter ignition delay due to a higher cetane number and an enhanced combustion process caused by oxygen in the biodiesel. On the other hand, the disadvantages of the biodiesel are higher kinematic viscosity and surface tension.

Biodiesel has lower heating value than mineral diesel and causes some loss of power. Therefore, it is necessary to increase the fuel amount to be injected into the combustion chamber. This will cause longer injection duration due to change in the injection timing. Higher cetane number corresponds to shorter ignition delay and advances the combustion timing [4].

In this paper the influence of biodiesel from rapeseed oil on combustion characteristics of bus diesel engine with M injection system is considered. Some important engine characteristics are determined by experiment and by numerical simulation. The objective is to identify as much as possible the dependences among fuel properties, the most important injection and combustion characteristics, harmful engine emissions, and other engine performances. Special attention is devoted to dependences among injection timing, in-cylinder gas temperature and NOX emission.

EXPERIMENTAL WORK AND NUMERICAL COMPARISON

The schematic diagram of the engine test bed is presented in **Fig.** Error! Reference source not found.. The test bed consists of an engine and electro-dynamometer Zöllner A-350AC, 300kW, air flow rate meter RMG, fuel consumption dynamic measuring system AVL, UHC analyser Ratfisch, NO_x chemoluminiscent analyzer Thermoelectron, O_2 analyzer Programmelectronic, CO analyzer Maihak, and smoke meter AVL. Using a data acquisition system the instantaneous injection pressure and needle lift, the instantaneous in-cylinder gas pressure, the temperatures of fuel, ambient air, intake air, cooling water at inflow and outflow of the engine, oil pressure and temperature, and the temperature exhaust gases are measured also.

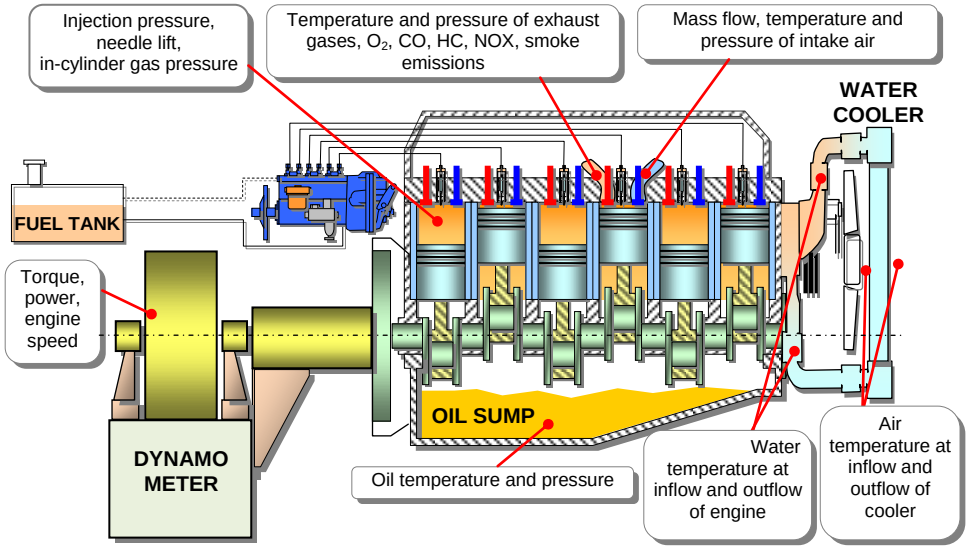

Figure 1 The engine test bed scheme.

The tested engine is a bus diesel engine MAN D 2566 MUM with a mechanically controlled fuel injection system. The engine has completed 500 000 km and has undergone general renovation. The direct injection M system is a kind of an injection combustion system. The M system does not distribute the fuel in the air initially, but sprays it with a single-hole nozzle onto the wall of a spherical combustion chamber, where it spreads to form a thin film. The fuel is injected in the direction of a high-speed air swirl. LabVIEW software platform is used to build the computer applications for data acquisition, data analyses and control algorithms. These applications are used to control the operation of the multifunction card and for data logging and post-processing.

The measurements and computations of engine characteristics are performed at various engine operating regimes. The comparison is done for all tested fuels at several operating regimes at full load, especially at the peak torque and rated conditions.

To check the accuracy of the numerical simulation used for our engine model, presented in **Fig.** Error! Reference source not found., the in-cylinder gas pressure, the engine power and the effective specific fuel consumption are measured at various engine operating regimes.

Accurate and efficient numerical analysis is a key factor for successful determination of combustion characteristics and their improvements. For the steady state performance prediction of diesel engines, there are several commercial packages that are widely accepted, rigorously tested, and verified. Efficient use of such software requires fine tuning of parameters and proper choice of available options. For the experiment approval in the presented case the AVL BOOST v2009.1 and the sub-models are used.

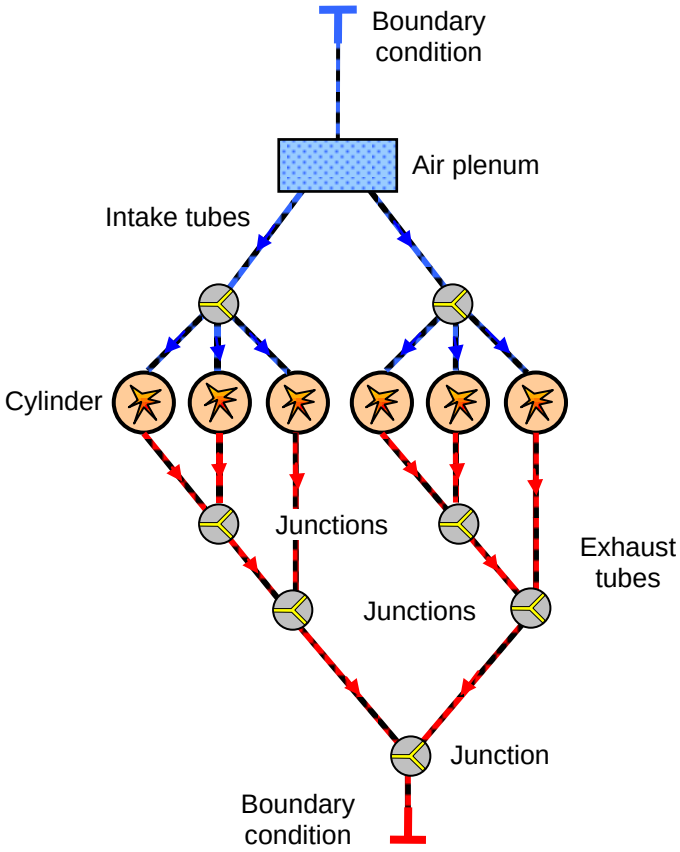

Figure 2 The engine model for numerical simulation

In-cylinder pressure is tested for both tested fuels at various operating regimes. **Fig.** Error! Reference source not found. show the comparison of the in-cylinder gas pressures, obtained numerically (AVL BOOST) and experimentally at rated condition by using B100 fuel and at peak torque condition when D2 fuel is used. A good agreement in the in-cylinder gas pressures at shows that the numerical simulation model is suitable to analyze the influence of B100 on combustion parameters. A similar agreement between experiment and numerical simulation was also obtained for engine power and effective specific fuel consumption.

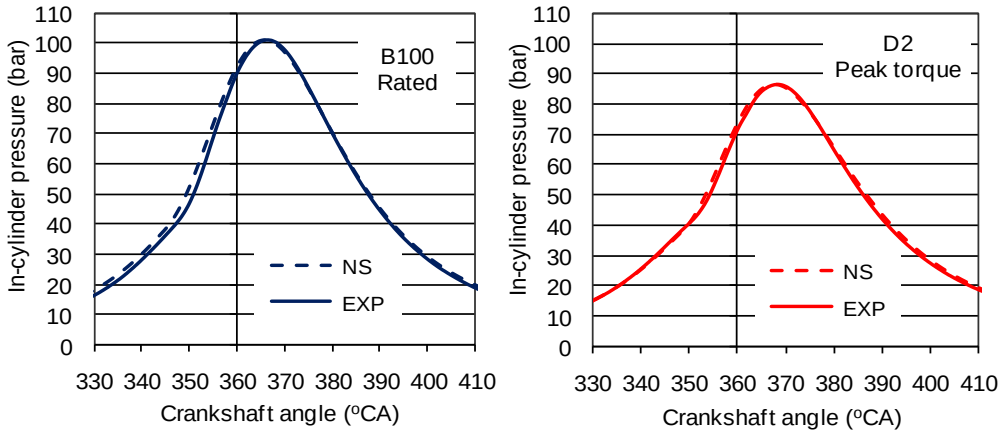

Figure 3 In-cylinder gas pressure at rated and peak torque conditions.

RESULTS AND DISCUSSION

To analyze the influence of fuel properties on bus diesel engine characteristics, the most important injection and combustion characteristics, obtained with B100 and D2, are compared and discussed in this chapter.

In-cylinder pressure is tested for both tested fuels at various operating regimes. **Fig.** Error! Reference source not found. show the comparison of the in-cylinder gas pressures, obtained numerically (AVL BOOST) and experimentally at rated condition by using B100 fuel and at peak torque condition when D2 fuel is used. A good agreement in the in-cylinder gas pressures at shows that the numerical simulation model is suitable to analyze the influence of B100 on combustion parameters. A similar agreement between experiment and numerical simulation was also obtained for engine power and effective specific fuel consumption.

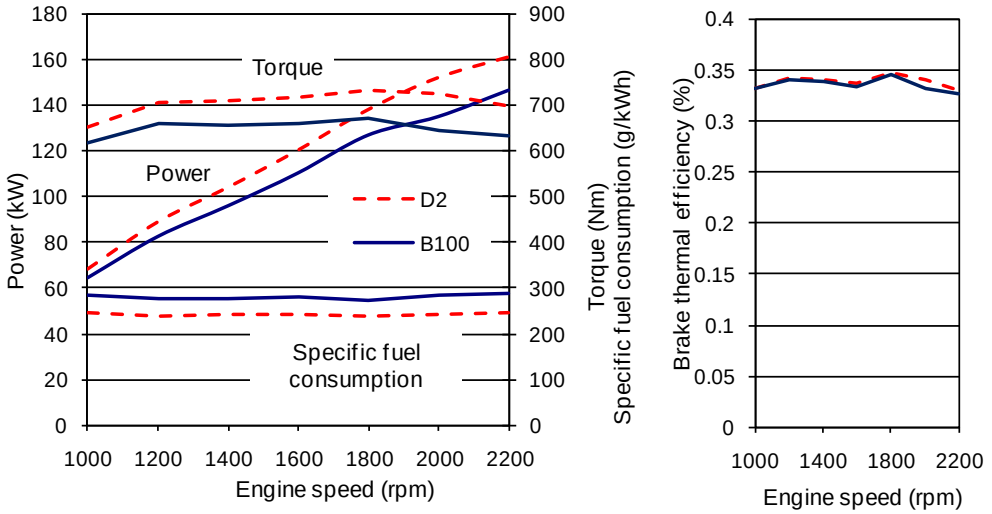

Figure 4 Effective power and torque, injected fuel mass and specific fuel consumption and brake thermal efficiency at full load conditions (numerical simulation).

Engine performance and harmful emissions are measured at various engine regimes. From the Fig. 4 the good agreement between numerical and experimental results is evident. B100 has lower effective power and torque by about 10 % and higher effective specific fuel consumption. The obvious reason is the lower heating value of B100.

Because the obtained power at the same operating regime is not the same for B100 and D2, the relative emissions are compared. Fig. **Error! Reference source not found.** presents the comparison of NOX, HC, CO, and smoke relative emissions, obtained experimentally. When B100 is used, NOX and HC relative emissions are higher; meanwhile CO and smoke relative emissions are lower. The differences of NOX relative emission between B100 and D2 are smaller at lower engine speeds.

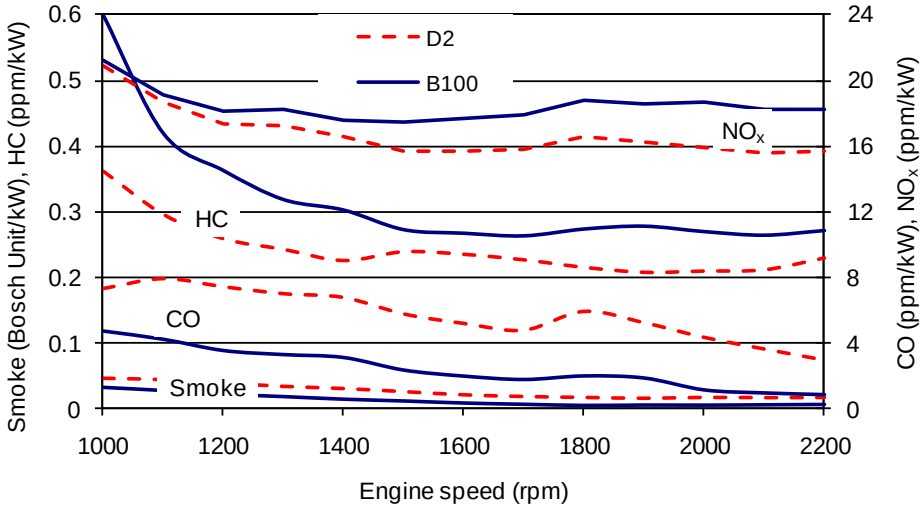

Figure 5 Relative emissions at full load conditions (experiment)

It is obvious that NOX relative emission generally increases with higher engine speed. This is partially due to the gas flow motion within cylinder under higher engine speed that leads to faster mixing between fuel and air and a shorter ignition delay. The reaction time of each engine cycle is reduced causing an earlier and higher in-cylinder gas temperature peak. By using B100 this effect is even more evident.

CONCLUSIONS

The influence of biodiesel produced from rapeseed oil (B100) on a bus diesel engine with direct fuel injection M system is investigated. By doing experiments and numerical simulation the relationships between fuel properties and engine emissions are analyzed.

- Higher density, viscosity, velocity of sound and bulk modulus of elasticity of B100 and lower vapor content in high pressure injection system cause the advanced injection timing and higher injection pressure.
- The advanced injection timing causes the increase of the in-cylinder gas pressure, in-cylinder gas temperature, and an earlier rise of the heat release rate.
- The higher injection pressure, higher oxygen content and other fuel properties of B100 results in lower smoke and CO emissions and in a slightly higher HC emission. The conditions in the cylinder during the first part of injection and combustion process

influence to a great extent the NOX formation. The results show that earlier appearance of temperature and heat release rate maximums prolongs the period with conditions favourable for NOX formation.

Thus, the higher NOX emission is a consequence of advanced injection and combustion process and of higher in-cylinder gas temperature at the beginning of combustion. The timing at which the maximum in-cylinder gas temperatures and heat release rates occur proved to be more important than the magnitude of the maximum temperature and maximum heat release rate.

ACKNOWLEDGMENT

This research was supported by the European Community's Sixth Framework Programme in the scope of the Civitas II Mobilis project.

REFERENCES

[1] Arsie I, Pianese C, Sorrentino M. Effects of control parameters on performance and emissions of HSDI diesel engines: Investigation via two zone modeling. Oil and Gas Scie and Technol 2007;62:457–469.
[2] Chan TL, Cheng XB. Numerical Modeling and experimental study of combustion and soot formation in a direct injection diesel engine. Energy Fuels 2007;21:1483–1492.
[3] Tree DR, Svensson KI. Soot processes in compression ignition engines. Prog in Energy and Combust Sci 2007;33:272–309.
[4] Canakci M. Combustion characteristics of a turbocharged DI compression ignition engine fueled with petroleum diesel fuels and biodiesel. Bioresour Technol 2007;98:1167–1175.
[5] Kegl B. Numerical analysis of injection characteristics using biodiesel fuel. Fuel 2006;85:2377–2387.

VARIABLE INTAKE VALVE LIFT ON A PORT FUEL INJECTED ENGINE AND ITS EFFECTS ON IDLE OPERATION

Adrian Clenci[1], Adrian Biziiac, Pierre Podevin, Rodica Niculescu

UDC:621

ABSTRACT: Reducing fuel consumption is a prime objective in the automotive industry in order to meet legal and customer demands due to the increasing price of oil. Variable valve actuation offers many opportunities for improving the spark ignition engine's performance in areas such as fuel economy and pollutant emissions.

This study presents a variable intake valve lift (ViVL) mechanism, used to enhance fuel economy in the area of idle operation and low part loads, which are the ones most frequently encountered in a vehicle's operation time. Currently, this mechanism is self-regulated thanks to a hydro-mechanical system and allows a continuous intake valve lift variation during engine operation.

Our studies revealed that the ability to control valve lift does indeed offer the ability to control intake air mass but also has the added benefit that it improves the fuel-air mixing process and controls air motion. This is particularly important at idle and low part loads when low lifts are to be used for improving the fuel economy or for achieving the required power.

The paper focuses on the experimental results obtained when approaching idle operation with different configurations of the intake valve timing system. Results indicating the potential of the ViVL system for fuel economy improvement, as well as results regarding the in-cylinder pressure evolution are presented in this paper.

Last but not least, the paper also presents a so-called Sleep&Start strategy, which can be seen as an alternative to the Stop&Start micro-hybridization solution. In other words, once a ViVL system has been installed on an engine, it should be used in every possible way in order to obtain a high benefits/cost ratio.

KEYWORDS: fuel economy, variable intake valve lift, combustion, idle operation

1 *Received August 2012, Accepted September 2012*

Intentionally blank

VARIABLE INTAKE VALVE LIFT ON A PORT FUEL INJECTED ENGINE AND ITS EFFECTS ON IDLE OPERATION

Adrian Clenci, Adrian Biziiac, Pierre Podevin, Rodica Niculescu

UDC:621

INTRODUCTION

As an energy source, from the standpoint of power density, stored energy and autonomy, the internal combustion engine still remains today an appropriate and attractive solution for ensuring mobility. Engines have improved dramatically over the past two decades, and they will continue to improve [18]. The current scientific developments described in [21] suggest that there could be 6–15% improvements in internal combustion fuel efficiency in the coming decade, although the filters required to meet emission legislation reduce these gains.

For quite some time, CO_2 emissions and their impact on the greenhouse effect have become a topic of debate [18]. In the late 1990s, the European, Japanese and Korean automotive manufacturers (ACEA, JAMA and KAMA) adopted a voluntary commitment to reduce average CO_2 emissions from new passenger cars sold to 140 g/km by 2008 with a view to reaching the EU target of 120 g/km by 2012 [18, 25]. In 2007, the European Commission underlined that progress had been made towards the 140 g/km target by 2008 but that the Community objective of 120 g CO_2/km would not be met by 2012 in the absence of additional measures. Therefore, in 2009, the EU laid down CO_2 emission performance standards through Regulation (EC) No 443/2009 [24]. This regulation stipulates that each OEM in the industry needs to achieve an average of 130 g CO_2/km by 2015 and 95 g CO_2/km by 2020 or face a punitive fine for exceeding the limits [23, 24].

Historically, engine selection for light vehicles consists in choosing either the spark ignition engine (SIE) or the compression ignition engine (CIE). While the diesel engine has made enormous progress in recent years and features good fuel economy, the gasoline engine still lags behind from this point of view. Of the two technologies, SIE is however the most likely to attract investment over the next decade. Already, many radical technical solutions (e.g. gasoline direct injection - GDI, variable valve actuation - VVA, variable compression ratio - VCR, Downsizing, Atkinson-Miller cycle) have been lately revealed and some have been applied in mass production [2, 3, 5, 8, 12, 13, 15, 16, 17, 21, 22]. Their purpose is to eliminate the inefficiencies that for the past century have largely been accepted as inevitable.

During most of its life, a passenger car engine is run under low loads and speeds. It is known that load reduction in SIE is traditionally accomplished by introducing additional losses during the intake stroke by means of a throttle plate. In these operating points, the overall engine efficiency decreases from the peak values (already not very high) to values that are dramatically lower (sometime even below 10%). An obvious conclusion would be to look for technical solutions able to offer better efficiency, such as throttle-free actuation, for instance.

Nowadays, two methods are being intensively investigated in order to obtain unthrottled operation: GDI, featuring load control by means of lean burn possibilities (see [22] or Mitsubishi GDI, VW FSI or Mercedes CGI), and VVA [2, 3, 5, 7, 8, 9, 10, 11, 12, 13, 15, 16, 17]. Both techniques promise a significant improvement in fuel economy.

However, only VVA still allows the use of the less expensive conventional exhaust gas after treatment (TWC), whereas lean GDI needs the more expensive extra treatment of nitrogen oxide (deNOx).

For some time there has been growing interest in throttle-less operation by means of VVA. Many scientific studies have been published on this subject, epitomized by BMW's Valvetronic-Vanos system, still the only continuously VVA system in mass production since 2001, able to offer throttle-less engine load control. According to papers [3, 16], a 15% fuel economy improvement was obtained on NEDC with a 1.8 litre engine.

Given this context, the paper presents a variable intake valve lift (ViVL) mechanism, used to enhance fuel consumption in the idle and low part loads operation [6, 7, 8, 9, 10, 11]. This mechanism is currently self-regulated thanks to a hydro-mechanical system, which is the subject of a French patent [19], and allows a continuous intake valve lift variation during engine operation, making throttle-less operation possible [9].

This study presents the initial experimental results obtained within the framework of several research contracts financed by the Romanian Council for Scientific Research (CNCSIS) and the French Agency for Research (OSEO-ANVAR) [9, 10, 11].

1. MECHANISM DESCRIPTION AND OPERATION

As can be seen from figure 1, the system comprises a side mounted camshaft and overhead valves, featuring a classical push-rod/rocker type mechanism. Spark ignition engines with the camshaft in the engine block (i.e. "push-rod engines") are still being built in the USA and are in use in even larger quantities throughout the world. This layout is low-end in design and can be produced at low cost [17].

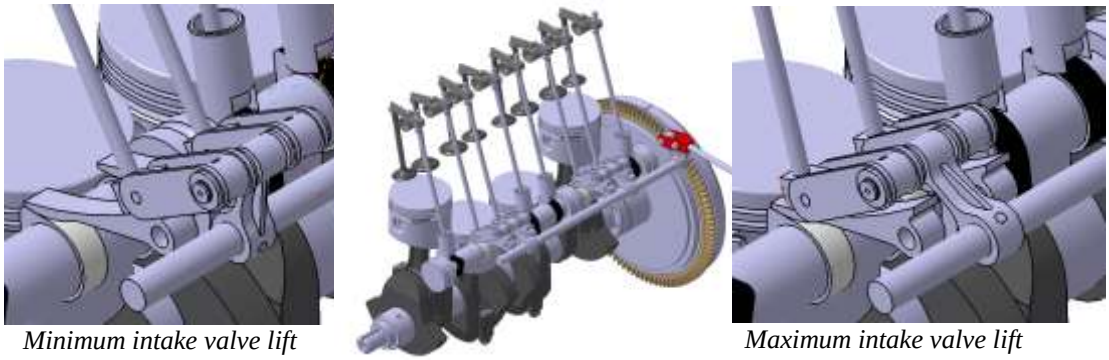

Minimum intake valve lift *Maximum intake valve lift*

Figure 1 The ViVL mechanism

The mechanism presented hereafter (figure 1) is able to adjust the intake valve lift thanks to an assembly consisting of an oscillating follower and a translational skate. The skate's position on the follower is adjusted with the help of a connecting rod and a control lever, so that every intake valve lift (iVL) can be achieved continuously between minimum and maximum values during operation. The control lever's position is given by a hydraulic cylinder, fed with oil from the engine's main oil gallery [5, 6, 7, 8, 9, 10, 11, 19].

The results of the intake valve displacement calculus as a function of cam rotation angle for different positions of the control lever are shown in figure 2. The ViVL mechanism also leads to variable valve overlap and opening duration through the thermal clearance, which induces a lost motion. A hydraulic lash adjuster could no doubt be used in

order to avoid having a non-controlled parameter, which is altered by the engine temperature, thus complicating the problem.

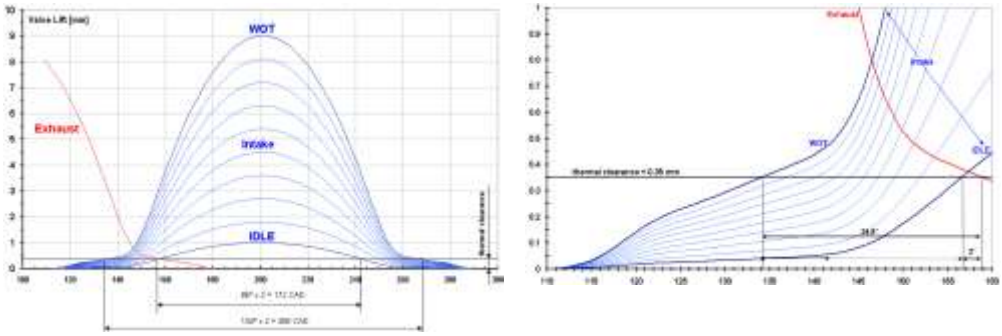

a. variable valve opening duration *b. variable valve overlap*

Figure 2 *Intake valve displacement*

The maximum intake valve law was imposed so as to be the same as the baseline engine from which this prototype originated, meaning that the goal is not to alter the engine operation at WOT but to improve it at low part loads and speeds. In the particular situation of using this ViVL mechanism, the unknown was the intake cam profile able to provide the maximum iVL mentioned above. An analytical synthesis was therefore performed. Afterwards, the partial intake valve laws corresponding to the part loads were obtained [6]. For the minimum iVL encountered at idle operation, the mechanism was designed to function if necessary at near-zero value. In this study, the minimum lift was set at 1 mm as it is stated in [16] that in most parts of the european driving cycle, the valve lift is below 1.5 mm and that a lift of 4 mm is reached only briefly in the higher speed part.

Mechanically speaking, ViVL provides some advantages particularly in the operating area corresponding to urban traffic (i.e. the most frequently encountered operation during the vehicle's lifetime):

- the lower the valve lift, the lower the spring force i.e. less energy is consumed to compress the springs;
- the lower the valve lift, the lower the energy lost to overcome the friction between the valve stems and their guides;
- the lower the valve lift, the lower the equivalent mass and force at the cam level (figure 3) [6].

These three features mean improved mechanical efficiency and engine reliability.

As concerns the latter, figure 4 presents the variation in equivalent mass at the cam level with the intake valve lift.

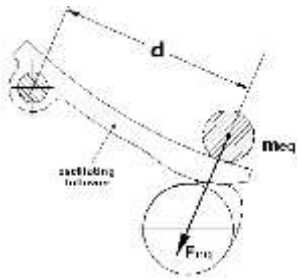

Figure 3
Equivalent mass on the cam level

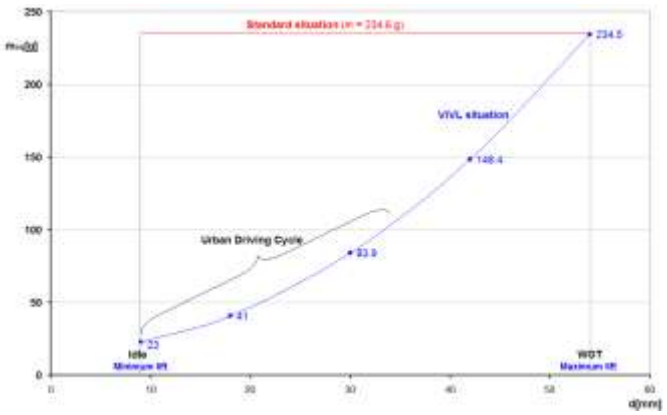

Figure 4 Equivalent mass at the cam level vs. intake valve law

Hence, it can be seen that at WOT the equivalent mass in the ViVL situation is equal to that of the standard system (i.e. without ViVL), while in the operating area specific to an urban driving cycle, the ViVL system provides much smaller values for the equivalent mass.

TEST BENCH RESULTS

The study was conducted on a 1.4 L, 4-cylinder in-line (77 mm stroke, 76 mm bore and geometric compression ratio 9), port-injected, spark ignition engine, which was equipped for acquiring the instantaneous in-cylinder pressure. Data acquisition and analysis of cycle-related parameters were performed with AVL Indimodul Hardware and AVL Concerto software. Engine testing was conducted over 200 complete engine cycles for each operating point. A p-V diagram displayed in real time was used to visually monitor combustion quality, which was judged statistically with the CoV of IMEP.

The parameters of the engine's injection and ignition management system were also modified in order to optimize the engine operation according to the new intake valve lift. Mapping, data acquisition and analysis were performed with INCA software.

Calibration of a standard engine management system is not an easy task and it already involves considerable engineering resources. Adding a new technology to a standard engine, such as the ViVL mechanism presented above, will introduce a greater level of complexity when addressing engine calibration. This is because of the additional degrees of freedom these systems come with. For example, an engine mapping, containing 2 main maps (one for the injection time map and the other one for the spark advance map) x 225 operating points, with 10 iVL will give 4500 points to analyze.

This paper presents the very first results of the attempt to optimize at stoichiometric value ($\lambda = 1$) the idle operation of the prototype engine with the new intake valve lift employed, i.e. the minimum one. It was decided to start with idle operation as this is where the maximum percentage improvement in fuel economy due to the use of low lifts is expected. All the tests were performed with the throttle plate closed, idle speed being achieved by correspondingly actuating the idle motor valve.

The reasons for not trying to approach idle with throttle-free operation are presented below. When considering gas exchange processes in the spark ignition engine, the goal is to conduct them so that the pumping losses are lower. As stated above, VVA could help in this direction (see the throttle-less load control). However, putting this idea into practice is quite challenging, especially at idle operation. For example, applying the strategy presented in figure 2 could ensure throttle-less load control but, as is also shown hereafter, it is accomplished at the expense of greater pumping losses, as the peak value of the intake valve lift needs to be quite low (<< 1 mm). In March 2006 [9], the prototype presented in figure 1 was able to operate unthrottled with a maximum intake valve lift of 0.5 mm but with an air excess of 1.6 (lean mixture); this means that to ensure stoichiometric operation, less air should be allowed to be drawn into the cylinder, which can be achieved by reducing even further the valve lift. If this strategy is chosen, pumping losses will increase even more.

A VVA strategy suited for unthrottled operation at part loads and that ensures smaller pumping losses consists in lowering the intake valve lift (not as much as before) with a highly restrained opening duration and in closing the intake valve very early. This is what BMW is doing thanks to its Valvetronic - BiVanos mechanism [2, 3, 16]. The problem with such a strategy is that once the intake valve closes, an expansion occurs during the rest of the intake stroke, which lowers the temperature (sometimes even to the limit of condensing the fuel) and diminishes the intake charge energy [3]. Greater velocity means greater energy, which accelerates combustion, and at idle operation, this phenomenon is very important as combustion stability is the key issue here. In order to avoid these phenomena, BMW operates at idle with late intake valve opening (LIVO) and a valve lift, which falls at 0.37 mm. This results in flow velocities approaching the speed of sound with a favourable effect on combustion. However, the pumping losses are greater than those obtained with the classical throttled engine, according to [3].

Therefore, one idea to emerge from this literature review is that even though minimal pumping losses should be one of the goals, this must not be done while impairing other aspects such as mixing process, charge kinetic energy prior to spark etc.

Thus, in this paper, two comparative situations were xperimentally explored: 850 rpm idle operation at maximum iVL vs. 850 rpm idle operation at minimum iVL, both at the same spark advance (12 CAD). For the minimum iVL, two other values for the spark advance (27 and 29 CAD) were subsequently tested in order to improve the engine operation even further.

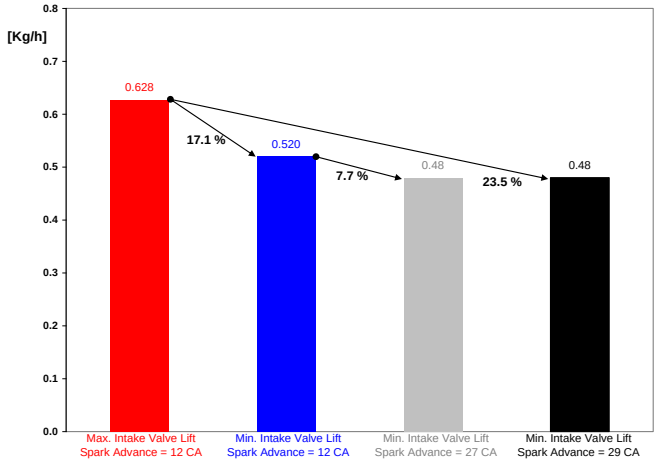

Figure 5 Fuel consumption results

Fuel consumption is shown in figure 5. Different reasons underpin these results, such as improvement of the fuel-air mixing process and air motion as the valve lift lowers. Moreover, as stated before, the energy to overcome the friction between the valve stems and their guides and the energy necessary to compress the valve springs decrease considerably as the lift lowers (e.g. between the maximum lift of 9 mm and the minimum one of 1 mm, the reduction in the energy necessary to compress the valve springs falls by almost 92 %). In order to differentiate between these two phenomena (the energetic one over the mechanical one), figure 9 presents eloquent results.

Increasing the spark advance from 12 to 27 or 29 CAD causes a further reduction in fuel consumption due to combustion, which occurs more around TDC.

In order to observe this in greater detail, figure 6, a and b shows typical indicated diagrams for the cases mentioned above. As the 27 CAD spark advance situation (the black dotted line in figure 6, a) is close to the 29 CAD spark advance situation (the black continuous line in figure 6, a), it was discarded from figure 6, b.

It can be seen that lowering the iVL leads to an increase in the pumping losses (figure 6, *b*). In fact, at 12 CAD spark advance, PMEP increased by about 5.8 % when running at idle with minimum iVL compared with the maximum lift. However, as seen in figure 5, there is a non-negligible fuel economy benefit in the minimum lift situation even in spite of increased pumping, meaning that the intensified flow speed underneath the intake valve (thus, the improved mixing process) and the reduced mechanical energy needed to compress the valve springs at lower lifts have strong effects upon the fuel consumption.

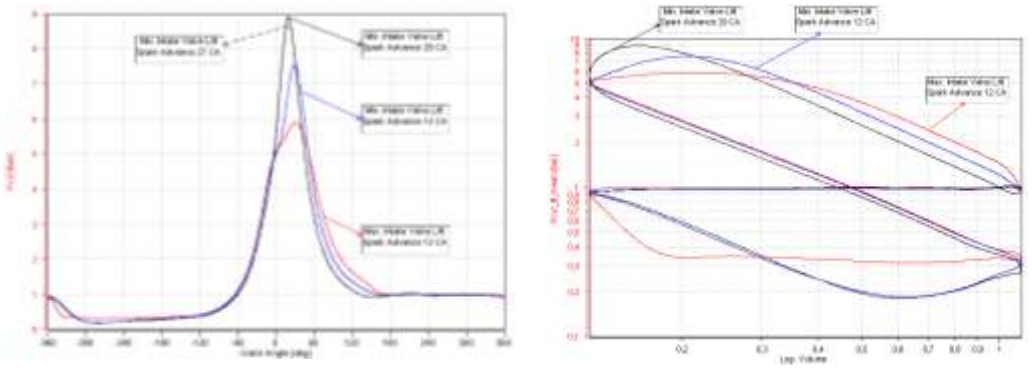

a. pressure over CA *b. LOG p – LOG V diagram*

Figure 6 Indicated diagrams at 850 rpm idle operation

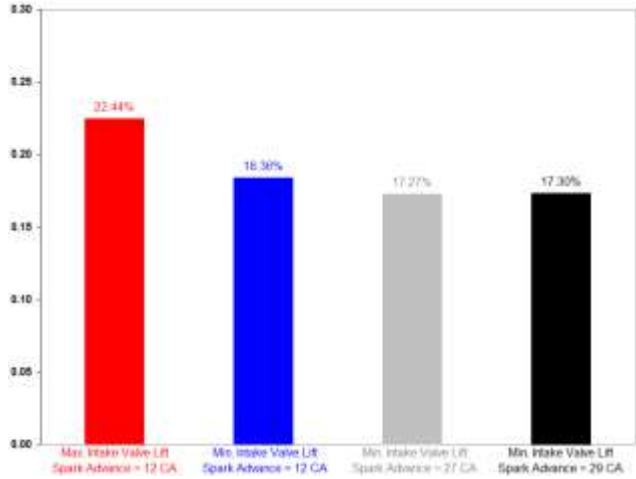

Figure 7 Engine filling efficiency

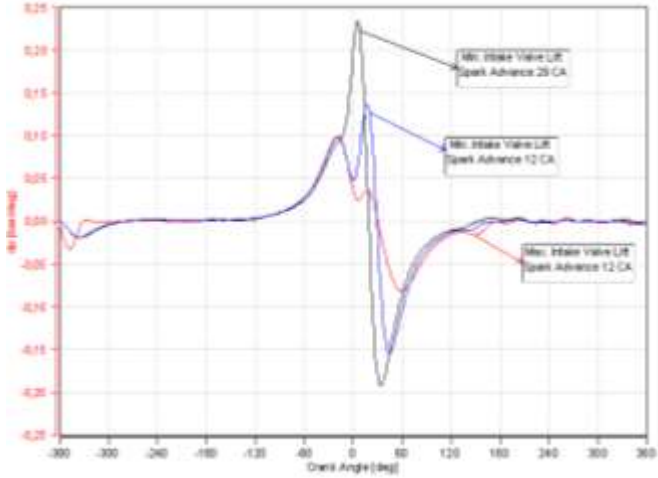

Figure 8 Pressure rise evolution over the CA

The effect of increasing PMEP can also be observed when analyzing the engine filling efficiency, which falls from 22.4 % at maximum iVL to 18.4 % at minimum iVL, both at the same 12 CAD spark advance (figure 7).

The peak pressure (figure 6, a) and, especially, the maximum pressure rise (figure 8) also increased significantly when using minimum lift, proving once again the virtues of a better mixing process and air motion. On the other hand, the two peaks of the pressure rise recorded at minimum valve lift with 12 CAD (blue curve in figure 8) indicate a small spark advance (combustion begins too late – see figures 9, 10 and table 1). Increasing the spark advance from 12 to 29 CAD, for instance, eliminated the two peaks mentioned before (black curve in figure 8).

Another advantage of operating with low lifts at idle operation is the reduction in the cyclic dispersion: CoV of IMEP decreased from 8.8 % to 5.4 % when passing from maximum to minimum lift at 12 CAD spark ignition advance and to 3.5 % at minimum lift and 29 CAD. This is also due to the reduction in the amount of internal EGR as the valve overlap decreases when the intake valve lift is lowered (figure 2, *b*).

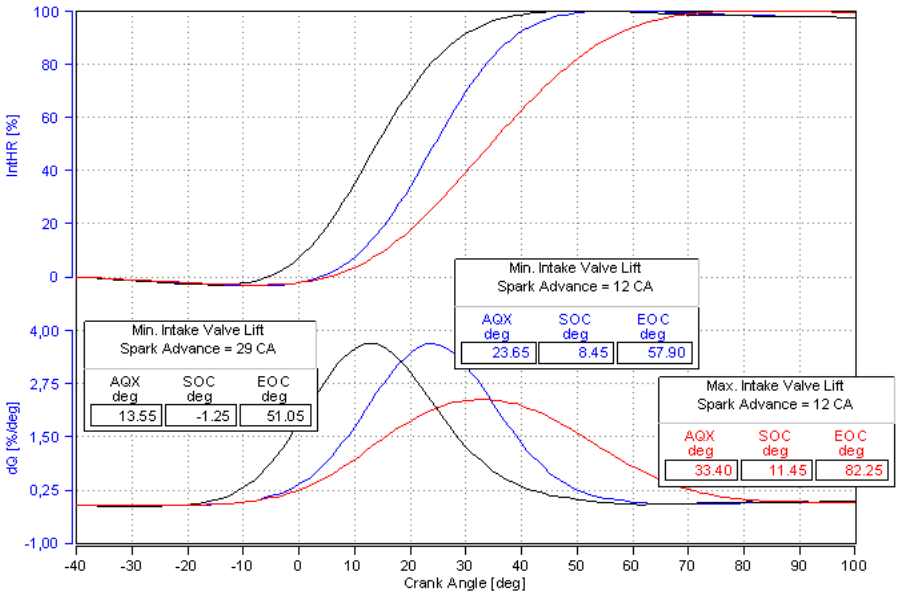

Figure 9 Heat release and rate of heat release evolutions

Figure 9 presents the heat release and rate of heat release evolution for the above-mentioned cases. Due to the difficulties in evaluating the convective coefficient, thermal losses to the engine walls were not considered, which means that the real end of combustion (EOC) cannot be found.

In figure 9, EOC is the moment when the zero value of the rate of heat release occurs. Conversely, the start of combustion (SOC) is conventionally taken as the moment when 5% mass burnt fraction takes place.

Figure 9 shows that with minimum lift, the heat release rate increases, which means that the main contributor to the fuel consumption reduction presented in figure 5 is the improvement in the air-fuel mixing process and air motion through lowering the valve lift.

To better assess combustion in the 3 cases considered, some more information is given in figure 10 and table 1.

Thus, when analyzing maximum iVL vs. minimum iVL at the same 12 CAD spark advance, it can be seen that the crank angle duration of all the combustion phases decreases, causing a better fuel economy, as seen in figure 5. As before, reducing the amount of internal EGR when lowering the intake valve lift is responsible for a more stable and faster combustion. When increasing the spark advance at the same minimum iVL, the combustion phase durations increase, which perhaps indicates a non-optimal value for the spark advance, though the fuel consumption still decreased (figure 5). Obviously, in order to clarify these aspects, there is a need for a more refined parametric study to determine the optimum spark advance for this particular operation.

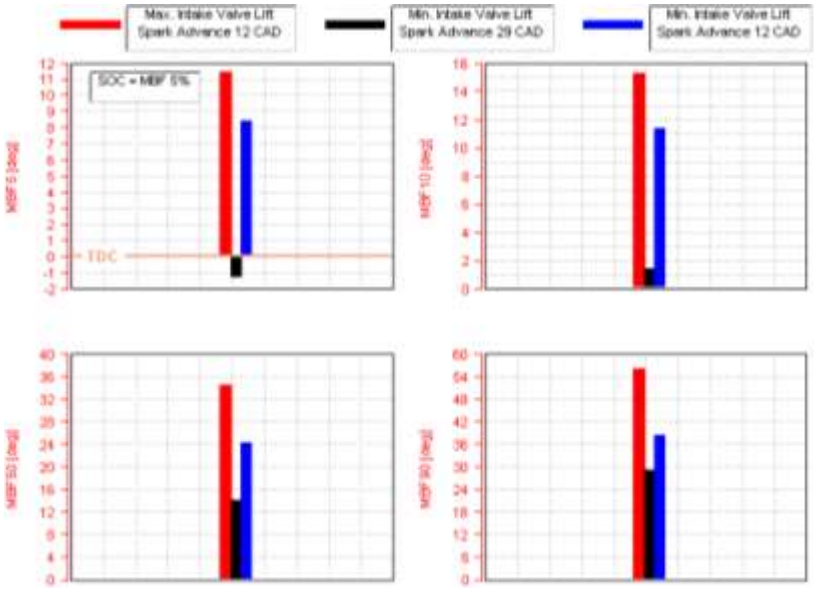

Figure 10 CAD at which some predefined per cent of energy is converted (5, 10, 50 and 90 %)

Table 1 Combustion phases' duration

Combustion phases	**Max. Intake Valve Lift**	**Min. Intake Valve Lift**	
	Spark Advance = 12 CAD	*Spark Advance = 12 CAD*	*Spark Advance = 29 CAD*
Ignition point – SOC	23.5	20.5	27.8
Ignition point – α_{pmax}	42.3	41	48
α_{pmax} – EOC	52	28.9	32.1
SOC – EOC	70.8	49.5	52.3

SLEEP&START STRATEGY

Idle operation is a prominent feature of real world driving, especially in congested city traffic. For vehicle homologation, standardised driving cycles are used. For instance, figure 11 presents the first portion of the NEDC/NMVEG cycle, corresponding to the urban driving cycle (UDC). This consists of four identical parts, which are said to represent city driving in Europe, having a total period of 240 seconds of idling (i.e. 31% of UDC total time).

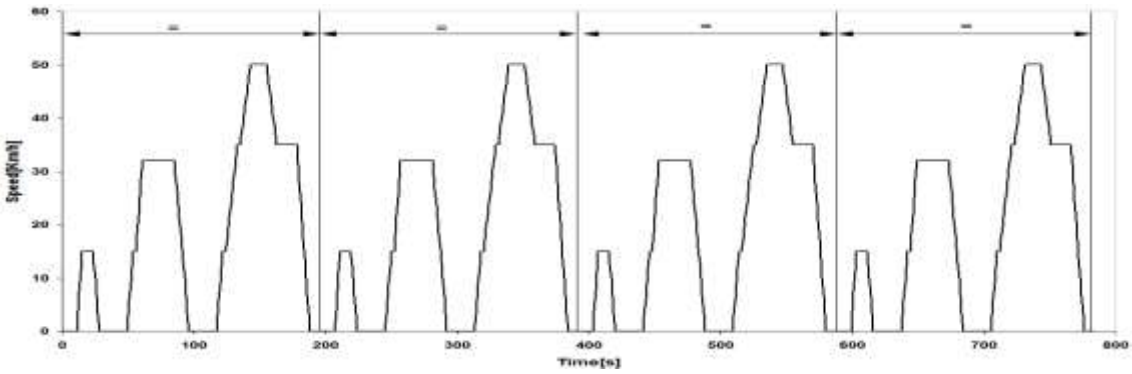

Figure 11 The UDC from the NEDC

In order to save fuel and thus to cut CO_2 emissions, currently the Stop&Start function is usually implemented on vehicles [1, 4, 14, 20, 21]. According to papers [1, 20, 21], a 5 to 10% potential in fuel economy on UDC can be attributed to this function.

The Stop&Start function marks the very first step toward hybridisation and is relatively straightforward. However, when implementing it on a vehicle some issues arise, which are briefly summarized below:

- the need for additional electric motors able to ensure HVAC within the stop phases;
- the need for a battery monitoring system, as SoC and SoH are the key issues in this area [10];
- the need to monitor the vacuum within the vehicle's assisted-braking system;
- the need to take into account the engine cool down during the stop phase;
- the need to have acceptable re-start times and vehicle acceleration from zero kmph.

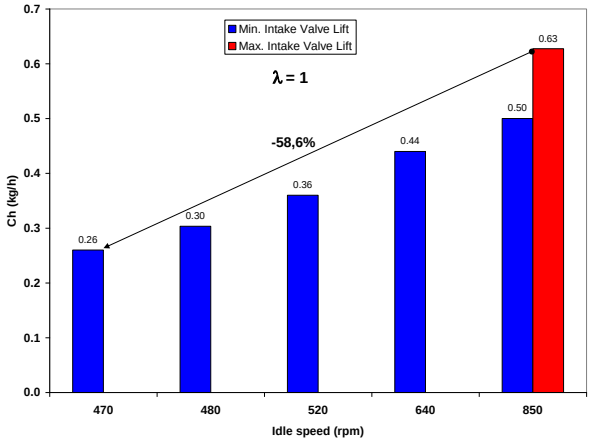

Figure 12 Fuel consumption reduction obtained by Sleep&Start strategy

In order to avoid the above problems, a so-called Sleep&Start strategy could be used, i.e. once an internal combustion engine features a ViVL system, the use of very low idle speeds could be envisaged the moment the vehicle has come to a stop.

In other words, once a ViVL system has been installed on an engine, it should be used in every possible way in order to obtain a high benefits/cost ratio.

The experiments on this particular matter showed that when idling at 470 rpm, at 1 mm intake valve lift and stoichiometric value, an almost 60% reduction was recorded with respect to the situation at 850 rpm and maximum intake valve lift (figure 12). The idle speed of 470 rpm was found to be the lowest limit at which proper cooling and lubrication were still possible using the same water and oil pumps as the standard engine. In fact, even though speeds lower than this could be obtained due to the low iVL, it seems they were insufficient to ensure a minimum water flow for the cooling needs of the engine.

If this strategy is applied only on the UDC, then 24.6 g of fuel is saved with respect to the standard situation illustrated in red in figure 12 (see the relation below):

$$FC_{Gain}\ [g] = \frac{Idle\_time_{UDC}\ [s] \cdot (C_{h\_standard\_idle} - C_{h\_Sleep\&Start})[Kg/h]}{3.6}$$

$$FC_{Gain} = \frac{240 \cdot (0.63 - 0.26)}{3.6} = 24.6\ g$$

If one takes as a reference the fuel consumption obtained on a UDC by a typical 5-door, C-class vehicle, which has a conventional 1.4 liter, 4-cylinder port-injected spark ignition engine, 75 hp and a 5-speed manual transmission with a kerb weight of 1130 kg, i.e. 277 grams of fuel, then the Sleep&Start strategy accounts for an 8.8% fuel reduction.

Within the context presented by this paper, the Sleep&Start strategy presents a certain interest in order to yield even greater fuel economy benefits from the ViVL mechanism.

3. CONCLUSIONS AND FUTURE WORK

In comparison with other solutions that might be considered as alternative automotive energy sources, the internal combustion engine still remains the most convenient option, and research efforts are currently being directed toward achieving increased efficiency throughout the entire automotive engine operating range.

In more than a century of spark ignition engine development, complete automatic regulation of air-fuel ratio and spark advance have been accomplished. Nowadays, taking into account the wide variety of the automotive engine's working regimes, the only way to obtain lower consumption and pollution is to provide the engine with automatic control systems such as the one presented in this paper. From this point of view, VVA offers many opportunities for improving the engine's performance in areas such as fuel economy and emissions, and it seems will become a must-have on gasoline engines.

This paper has presented the initial experimental results obtained when approaching idle operation with different configurations of the intake valve timing system. These results revealed an improvement in fuel economy at idle operation of around 20% in spite of an increased pumping work. As stated, this gain in fuel economy was mainly generated by an increased airflow velocity of the fresh mixture into the cylinders, causing an improvement in the fuel-air mixing process and, in the end, better combustion. Thus, one could say this is the most significant element in the equation of fuel consumption reduction at idle operation.

Moreover, additional work is still to be performed in order to ascertain the full potential of ViVL for fuel economy, such as more refined parametric studies in order to map the injection and ignition management system for each iVL from the whole operating engine field.

ACKNOWLEDGMENTS

This paper is the result of a team effort.

The authors would like to express their gratitude to the Romanian Council for Scientific Research in Higher Education (CNCSIS-CEEX), as well as to the Agence Nationale de Valorisation de la Recherche (Oseo-ANVAR) for their financial support.

Thanks are also due to Mr. Eric Pain and Mr. Julien Berquez from Renault Technologie Roumanie for providing the necessary hardware for the engine calibration and to AVL Gmbh Austria for their contribution regarding the experimental setup.

ABBREVIATIONS

ACEA – Association des Constructeurs Européens d'Automobiles;
AQX – crank angle at which the rate of heat release is maximal;
CA – crank angle;
CAD – crank angle degrees;
CGI – charge guided injection;
CIE – compression ignition engine;
C_h – hourly fuel consumption, [Kg/h]
d – skate's displacement on the oscillating follower, [mm]
EC – European Commission;
EGR – exhaust gas recirculation;
EOC – end of combustion;
EU – European Union;
$FC_{\_gain}$ – fuel consumption gain, [g]
FSI – fuel stratified injection;
GDI – gasoline direct injection;
HR – heat release;
HVAC – heating-ventilation and air-conditioning;
IMEP – indicated mean effective pressure;
iVL – intake valve lift, [mm];
JAMA – Japanese Automobile Manufacturers' Association;
KAMA – Korean Automobile Manufacturers' Association;
MBF – mass burnt fraction;
m_{eq} – equivalent mass at the cam level, [g]
NEDC – New European Driving Cycle;
OEM – original equipment manufacturers;
PMEP – pumping mean effective pressure;
SIE – spark ignition engine;
SoC – state of charge;
SoH – state of health;
TDC – top dead center;
TWC – three way catalyst;
UDC – urban driving cycle;
VCR – variable compression ratio;
ViVL – variable intake valve lift;
VVA – variable valve actuation;
WOT – wide open throttle.

REFERENCES

[1] Badin, F. – La voiture hybride, Conférence INRETS, CNAM, Paris, juin 2007
[2] Begg, S.M., Hindle M.P., Cowell T., Heikal M.R. – Low intake valve lift in a port fuel-injected engine, Energy, Volume 34, Issue 12, Pages 2042-2050, December 2009
[3] Bernhard, L. – Less CO2 thanks to the BMW 4 cyl. Valvetronic engine, ATA vol. 56, no 3-4/2003.
[4] Bitsche, O., Gutmann, G. - Systems for hybrid cars, Journal of Power Sources 127 (2004) 8–15
[5] Bîzîiac, A., Clenci, A., Podevin, P. - Intêrets et enjeux de la distribution variable, 8ème Cycle de conférences CNAM/SIA retransmises par visioconférence sur des sites distants, Paris 2007
[6] Clenci, A., Bîzîiac, A., Podevin, P., Descombes, G., Hara, V. - Synthesis and analysis of a variable valve lift and timing mechanism, 1st International Congress on Automotive, AMMA2007, held in Cluj-Napoca, Romania, under the patronage of FISITA.
[7] Clenci, A., Podevin, P., Bîzîiac, A., Descombes, G., Hara, V. - Development of a variable valve lift and timing system for low part loads efficiency improvement, EAEC Congress, 2007, Budapest, Hungary
[8] Clenci A., Descombes G., Podevin P., Hara V. – Some aspects concerning the combination of downsizing with turbocharging, variable compression ratio and variable intake valve lift, Proceedings of the Institution of Mechanical Engineers Part D, October 2007, ISSN 0954-4070, Journal of Automobile Engineering, London, England
[9] Clenci, A. et al - Spark ignition engine featuring a variable valve lift and timing (VVLT) system, which allow the throttle-less operation, Research contract no. At 140, granted by CNCSIS, 2005 – 2006, Romania
[10] Clenci, A. et al - Ecological Vehicle by Intake Throttle-less Actuation (EcoVITA), Research contract no. Et 608, granted by CNCSIS-CEEX, 2006 – 2008, Romania
[11] Clenci, A., Podevin, P. et al - Moteur avec autorégulation de la levée des soupapes d'admission. Mise au point du système de contrôle de levée de soupapes, Projet de recherche Oseo-Anvar France, 2008
[12] Fontana, G., Galloni, E. – Variable valve timing for fuel economy improvement in a small spark-ignition engine, Applied Energy 86 (2009) 96–105
[13] Hannibal, W., Flierl, R., Stiegler, L., Meyer, R. – Overview of current continuously variable valve lift systems for four-stroke spark-ignition engines and the criteria for their design ratings, SAE Paper 2004-01-1263
[14] Karden, E. et al - Requirements for future automotive batteries – a snapshot, Journal of Power Sources 144 (2005) 505–512
[15] Kreuter, P., Heuser, P., Reinicke-Murmann, J., Erz, R., Ulrich, P., Böcker, O – Variable Valve Actuation – Switchable and Continuously Variable Valve Lifts, SAE Paper 2003-01-0026.
[16] Liebl, J., Poggel, J, Klutting, M., Missy, S. – Der neue BMW Ottomotor mit Valvetronic, MTZ Motortechnische, 62, 2001
[17] Mohr, M., Flierl, R., Hannibal, W. – Potential of a Mechanical Fully Variable Valve Lift System for Engines with a Side-Mounted Camshaft, SAE Paper 2004-01-1395.
[18] Plotkin, S. E. – Examining fuel economy and carbon standards for light vehicles, Energy Policy 37 (2009) 3843–3853
[19] Podevin, P., Descombes, G., Clenci, A., Hara, V., Boncea, S. - Procédé de régulation d'une levée de soupape, dispositifs de soupape à ouverture variable, moteur équipé d'un tel dispositif, Brevet d'Invention français, n°FR2883927, octobre 2006

[20] Vangraefschepe, F., Menegazzi, P. - Véhicules hybrides, quel avenir ?, www.ifp.fr (Panorama 2005)
[21] Taylor, A. – Science review of internal combustion engines, Energy Policy 36 (2008) 4657–4667
[22] Yousef S.H Najjar – Comparison of performance of a greener direct-injection stratified-charge (DISC) engine with a spark-ignition engine using a simplified model, Energy, Volume 36, Issue 7, Pages 4136-4143, july 2011
[23] Wells, P., Morreau S. – From 10:10 to 50:50 – OEMs face the CO2 challenge, AutomotiveWorld.com, 2011
[24] www.eur-lex.europa.eu
[25] http://ec.europa.eu/environment/air/transport/co2/co2_agreements.htm

MVM – International Journal for Vehicle Mechanics, Engines and Transportation Systems

NOTIFICATION TO AUTHORS

The Journal MVM publishes original papers which have not been previously published in other journals. This is responsibility of the author. The authors agree that the copyright for their article is transferred to the publisher when the article is accepted for publication.

The language of the Journal is English.

Journal ***Mobility & Vehicles Mechanics*** is at the SSCI list.

All submitted manuscripts will be reviewed. Entire correspondence will be performed with the first-named author.

Authors will be notified of acceptance of their manuscripts, if their manuscripts are adopted.

INSTRUCTIONS TO AUTHORS AS REGARDS THE TECHNICAL ARRANGEMENTS OF MANUSCRIPTS:

Abstract is a separate Word document, "*First author family name_ABSTRACT.doc*". Native authors should write the abstract in both languages (Serbian and English). The abstracts of foreign authors will be translated in Serbian.

This document should include the following: 1) author's name, affiliation and title, the first named author's address and e-mail – for correspondence, 2) working title of the paper, 3) abstract containing no more then 100 words, 4) abstract containing no more than 5 key words.

The manuscript is the separate file, „*First author family name_Paper.doc*" which includes appendices and figures involved within the text. At the end of the paper, a reference list and eventual acknowledgements should be given. References to published literature should be quoted in the text brackets and grouped together at the end of the paper in numerical order.

Paper size: Max 16 pages of B5 format, excluding abstract
Text processor: Microsoft Word
Margins: left/right: mirror margin, inside: 2.5 cm, outside: 2 cm, top: 2.5 cm, bottom: 2 cm
Font: Times New Roman, 10 pt
Paper title: Uppercase, bold, 11 pt
Chapter title: Uppercase, bold, 10 pt
Subchapter title: Lowercase, bold, 10 pt
Table and chart width: max 125 mm
Figure and table title: Figure _ (Table _): Times New Roman, italic 10 pt

Manuscript submission: application should be sent to the following e-mail:

mvm@kg.ac.rs ; lukicj@kg.ac.rs
or posted to address of the Journal:
University of Kragujevac – Faculty of Engineering
International Journal M V M
Sestre Janjić 6, 34000 Kragujevac, Serbia

The Journal editorial board will send to the first-named author a copy of the Journal offprint.

MVM – International Journal for Vehicle Mechanics, Engines and Transportation Systems

OBAVEŠTENJE AUTORIMA

Časopis MVM objavljuje orginalne radove koji nisu prethodno objavljivani u drugim časopisima, što je odgovornost autora. Za rad koji je prihvaćen za štampu, prava umnožavanja pripadaju izdavaču.

Časopis se izdaje na engleskom jeziku.

Časopis ***Mobility & Vehicles Mechanics*** se nalazi na SSCI listi.

Svi prispeli radovi se recenziraju. Sva komunikacija se obavlja sa prvim autorom.

UPUTSTVO AUTORIMA ZA TEHNIČKU PRIPREMU RADOVA

Rezime je poseban Word dokument, "*First author family name_ABSTRACT.doc*". Za domaće autore je dvojezičan (srpski i engleski). Inostranim autorima rezime se prevodi na srpski jezik. Ovaj dokument treba da sadrži: 1) ime autora, zanimanje i zvanje, adresu prvog autora preko koje se obavlja sva potrebna korespondencija; 2) naslov rada; 3) kratak sažetak, do 100 reči, 4) do 5 ključnih reči.

Rad je poseban fajl, „*First author family name_Paper.doc*" koji sadrži priloge i slike uključene u tekst. Na kraju rada nalazi se spisak literature i eventualno zahvalnost. Numeraciju korišćenih referenci treba navesti u srednjim zagradama i grupisati ih na kraju rada po rastućem redosledu.

Dužina rada: Najviše 16 stranica B5 formata, ne uključujući rezime
Tekst procesor: Microsoft Word
Margine: levo/desno: mirror margine; unurašnja: 2.5 cm; spoljna: 2 cm, gore: 2.5 cm, dole: 2 cm
Font: Times New Roman, 10 pt
Naslov rada: Velika slova, bold, 11 pt
Naslov poglavlja: Velika slova, bold, 10 pt
Naslov potpoglavlja: Mala slova, bold, 10 pt
Širina tabela,dijagrama: max 125 mm
Nazivi slika, tabela: Figure __ (Table _): Times New Roman, italic 10 pt

Dostavljanje rada elektronski na E-mail: **mvm@kg.ac.rs ; lukicj@kg.ac.rs**

ili poštom na adresu Časopisa
Redakcija časopisa M V M
Fakultet inženjerskih nauka
Sestre Janjić 6, 34000 Kragujevac, Srbija

Po objavljivanju rada, Redakcija časopisa šalje prvom autoru jedan primerak časopisa.

MVM *Editorial Board*
University of Kragujevac
Faculty of Engineering
Sestre Janjić 6, 34000 Kragujevac, Serbia
Tel.: +381/34/335990; Fax: + 381/34/333192
www.mvm.fink.rs